

## Lehigh University Lehigh Preserve

---

### Theses and Dissertations

---

1996

# Dynamic analysis of the interface stress and spallation in coated materials

Jong-ho Kim  
*Lehigh University*

Follow this and additional works at: <http://preserve.lehigh.edu/etd>

---

### Recommended Citation

Kim, Jong-ho, "Dynamic analysis of the interface stress and spallation in coated materials" (1996). *Theses and Dissertations*. Paper 406.

This Thesis is brought to you for free and open access by Lehigh Preserve. It has been accepted for inclusion in Theses and Dissertations by an authorized administrator of Lehigh Preserve. For more information, please contact [preserve@lehigh.edu](mailto:preserve@lehigh.edu).

**Kim, Jung-ho**

**Dynamic Analysis  
of the Interface  
Stress and  
Spallation in Coated  
Materials**

**June 2, 1996**

Dynamic Analysis of the Interface Stress and  
Spallation in Coated Materials

by

Jung-ho Kim

A Thesis

Presented to the Graduate and Research Committee

of Lehigh University

in Candidacy for the Degree of

Master of Science

in

Applied Mechanics

Lehigh University

April, 1996

This thesis is accepted and approved in partial fulfillment of the requirements for the Master of Science.

Date: 4/25/1996

Thesis Advisor:

Chairperson of Department:

## Table of Contents

Chapter	Page
Abstract	1
1. Introduction	2
2. Formulation of Problem and Solution	6
3. Results and Discussion	17
4. Conclusion	55
References	56
Biography	58

## List of Tables

Table	Page
1. Elastic Constants of Brass and Copper	27
2. Elastic Constants of Aluminum and Epoxy	40

## List of Figures

Figure	Page
1. Element of Rod Displaced by a Longitudinal Wave	6
2. A Slender Two-Part Composite Rod	9
3. Stress Wave Behavior in a Two-Part Composite Rod	26
4. Stress Distribution on the Interface(Materials: 1 Brass, 2 Copper, $n=0$ )	29
5. Stress Distribution on the Interface(Materials: 1 Brass, 2 Copper, $n=1$ )	30
6. Stress Distribution on the Interface(Materials: 1 Brass, 2 Copper, $n=5$ )	31
7. Stress Distribution on the Middle of Material 2(Materials: 1 Brass, 2 Copper, $n=5$ )	32
8. Stress Intensity Factors and the Strain Energy Release Rate for a Penny-Shaped Interface Crack(Materials: 1 Aluminum, 2 Epoxy)	40
10. Stress Distribution on the Interface(Materials: 1 Aluminum, 2 Epoxy, $n=1$ )	42
11. Stress Distribution on the Interface(Materials: 1 Aluminum, 2 Epoxy, $n=2$ )	43

12. Stress Distribution on the Interface(Materials: 1 Aluminum, 2 Epoxy, n=3)	44
13. Stress Distribution on the Interface(Materials: 1 Aluminum, 2 Epoxy, n=4)	45
14. Stress Distribution on the Interface(Materials: 1 Aluminum, 2 Epoxy, n=5)	46
15. Stress Distribution on the Interface(Materials: 1 Aluminum, 2 Epoxy, n=6)	47
16. Stress Distribution on the Interface(Materials: 1 Aluminum, 2 Epoxy, n=7)	48
17. Stress Distribution on the Interface(Materials: 1 Aluminum, 2 Epoxy, n=8)	49
18. Stress Distribution on the Interface(Materials: 1 Aluminum, 2 Epoxy, n=9)	50
19. Stress Distribution on the Interface(Materials: 1 Aluminum, 2 Epoxy, n=10)	51
20. Partly Magnified Plot of Fig.19	52
21. Stress Distribution at $x=h_2/10$ (Materials: 1 Aluminum, 2 Epoxy, n=10)	53
22. Stress Distribution at $x=-h_2/10$ (Materials: 1 Aluminum, 2 Epoxy, n=10)	54



## Abstract

In this thesis a simple, two-part piecewise homogeneous composite medium subjected to an impulsive loading is considered to analyze the reflection and transmission of stress waves in the system. The system is governed by the well known wave equation and the Laplace transform method is employed to obtain an accurate short-time response to the load. The solution obtained is in the form of an infinite series. By applying the image method to the final solution, easily understandable step by step analysis is performed to describe the wave propagation within the system. Several results obtained by substituting properties of existing materials in the final solution are presented. Also, for a more practical application, the spallation problem of an elastic layer bonded to a different material having a crack on the interface is considered.

# 1. Introduction

Stress-wave propagation in metallic and non-metallic materials has been studied extensively in the past to examine mechanical behavior. Earlier, in his book entitled *Stress Wave in Solids*, Kolsky[1] presented both a theoretical and experimental account of wave propagation in solids in elastic and dissipative media\*. A stress wave technique was used to determine the tensile strength of alumina by Abbott and Cornish[2]. They gave experimental evidence to verify the reliability of the state of dynamic tensile stress resulting from the reflection of a longitudinal stress wave from a free boundary. Abbott and Broutman[3] carried out experiments to observe phenomena of longitudinal stress-wave propagation in composites. The plane strain problem for the bonded medium which is composed of three different materials and which contains an interface crack was solved by Erdogan and Gupta[4]. The primary interest in this problem was on the analysis of the

\* Numbers in brackets refer to references given at the end of the thesis

disturbed stress state caused by the interface crack. The axially symmetric elasticity problem for a layer bonded to two half spaces of different mechanical properties and containing a penny-shaped crack lying parallel to the interface at an arbitrary location was solved by Arin and Erdogan[5]. They presented the numerical results showing the effect of the ratio of the layer thickness to the crack length on the stress intensity factors and the strain energy release rate. Arin and Erdogan[6] solved axially symmetric elastostatic problem for an elastic layer bonded to a half space and containing a penny-shaped crack on the interface. The solution of this problem is very useful as an approximation to the delamination problem caused by the reflected stress waves in layered materials. Recently, Gupta, Yuan and Pronin[7] presented useful applications of laser spallation technique to measure the interface strength between several different coatings and substrates. In the laser technique, the critical stress amplitude that accomplishes the removal of the coating was determined. In addition to those mentioned above, many others have investigated stress-wave behavior because a stress pulse with sufficiently large amplitude traveling through a solid may produce fractures.

The fractures produced by stress pulses differ from those produced

statically for several different reasons. Among those, one which is very closely related to the purpose of this study is when a compression pulse is incident on a free boundary, it gives rise to a reflected tension pulse, which, when reflected obliquely, would produce both a dilatational and a distortional pulse. The interference of such reflected pulses may give rise to very complicated stress distributions and the superposition of several reflected pulses may produce stresses which are sufficiently large to cause fracture when the amplitude of the incident pulse was too small to do so. So, stress-wave analysis is a powerful tool for studying the mechanical properties of newly developed materials, especially for study of mechanical properties of interfaces between different materials.

It is critical to determine the stress distribution on the interfaces between different materials because often stress concentrations occur right on the interfaces and cause failure. There are large number studies that investigate the stress distribution on the interfaces by using several different methods. In this study mathematical simulation method is used to observe one-dimensional stress-wave propagation in a freely supported prismatic two-part composite rod. A rectangular pulse is applied to one stress-free end of a long, thin, freely supported prismatic rod. It is assumed that the

amplitude of the applied stress pulse is known. For simplicity a number of additional assumptions are made. It is assumed that the actual physical problem may be represented by a one-dimensional wave equation, that is, plane parallel sections remain plane and parallel during deformation and lateral inertia effects associated with contraction-expansions due to the Poisson effect is neglected. In this study the Laplace transform method rather than the standard normal mode method is used. As a consequence the predicted response which is in the form of an infinite series tends to converge very fast for relatively short values of time. The comparison of these two methods is well presented by Graff[8] in his book entitled Wave Motion in Elastic Solids.

The stress distribution on the interface between different materials is useful to determine failure initiation. In the last part of this study a practical application of the stress analysis to a delamination problem is included.

## 2. Formulation of the Problem and Solution

The main goal of this section is to obtain an expression of stress-state for a composite rod or a coated plate. To accomplish this, first the equation of motion of a prismatic slender rod will be derived. Then the exact stress distribution will be obtained by making use of the boundary conditions for the interface and the free end.

Consider a long, slender rod as shown in Fig.1.

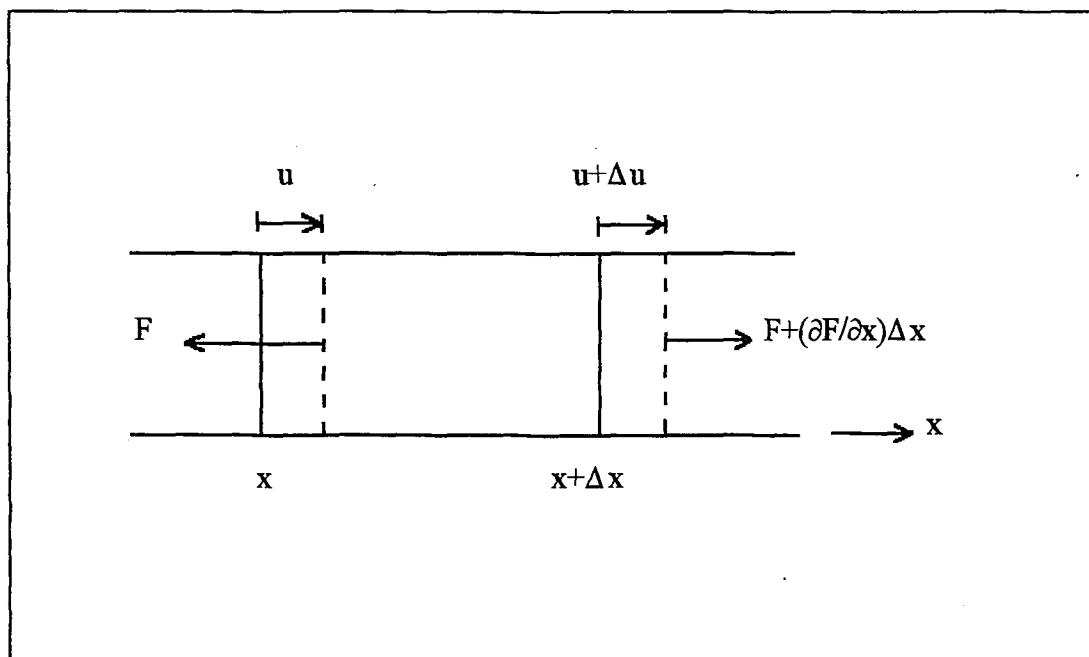


Fig.1 Element of rod displaced by a longitudinal wave

It is assumed that the rod has a constant cross-sectional area  $A$ , a uniform mass density  $\rho_0$ , a Young's modulus  $E$ , and the rod is sufficiently slender to permit us to neglect radial motion, arising from radial extension coupled through Poisson's ratio to the axial displacement. According to the work done by Abbott and Cornish[2], if the lateral dimension of the rod is less than about 1/10 the wavelength of the impulse, and the impulse pressure is uniformly distributed over the end, then an unchanging longitudinal wave will propagate along the rod. Referring to Fig. 1, we see that when a longitudinal wave is present, a plane at  $x$  moves to  $x+u$  and a neighboring plane at  $x+\Delta x$  moves to  $x+\Delta x+u+\Delta u$ . The element of the rod between these planes, having the mass  $A\rho_0\Delta x$ , is acted upon by the tensile force  $F$  at its left end and by the tensile force  $F+(\partial F/\partial x)\Delta x$  at its right end, as shown. Since the net force on the element in the positive direction is  $(\partial F/\partial x)\Delta x$ , Newton's second law requires that

$$\frac{\partial F}{\partial x}\Delta x = A\rho_0\Delta x\frac{\partial^2 u}{\partial t^2} \quad (1)$$

By the definition of Young's modulus, the tensile force  $F$  and the strain  $\partial u/\partial x$  are related by the equation

$$F = AE \frac{\partial u}{\partial x} \quad (2)$$

On introducing this expression for F into (1) and canceling  $A \Delta x$ , we are left with the wave equation

$$\frac{\partial^2 u}{\partial x^2} = \frac{1}{c_0^2} \frac{\partial^2 u}{\partial t^2} \quad (3)$$

where the wave velocity for longitudinal wave is

$$c_0 = \sqrt{\frac{E}{\rho_0}} \quad (4)$$

Note that the one dimensional wave equation (3) is valid also for the propagation of irrotational plane waves in a medium which is very large in y and z directions provided the wave velocity  $c_0$  is calculated from  $c_0 = [(\lambda + 2\mu)/\rho_0]^{1/2}$ , where  $\lambda$  and  $\mu$  are Lamé's constants.

Now we proceed to the main problem. Consider a simple two-part composite rod as shown in Fig.2. It is presumed that the rod is different in length and material. The wave equation obtained in (3) governs the system,



$$\frac{\partial^2 u_1(x,t)}{\partial x^2} = \frac{1}{c_1^2} \frac{\partial^2 u_1(x,t)}{\partial t^2}$$

$$\frac{\partial^2 u_2(x,t)}{\partial x^2} = \frac{1}{c_2^2} \frac{\partial^2 u_2(x,t)}{\partial t^2} \quad (5)$$

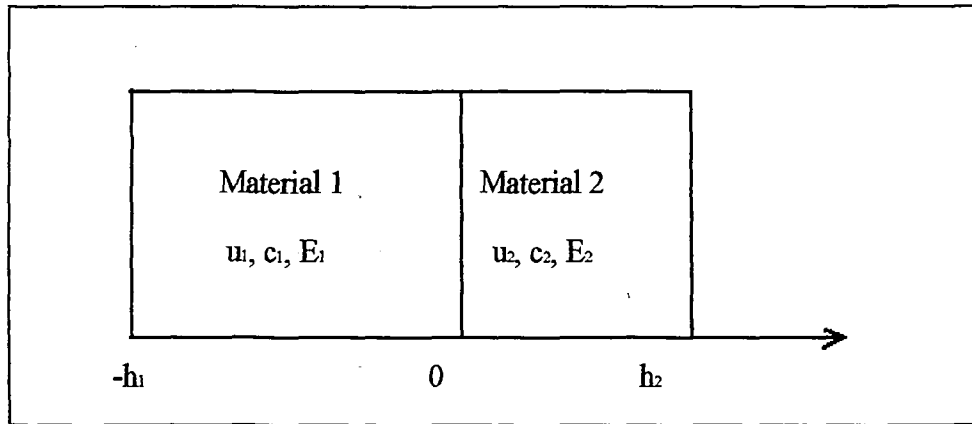


Fig.2 A slender two-part composite rod

The coordinate  $x$  refers to the axis of the rod, while the longitudinal displacement is given by  $u(x,t)$ .  $c_1, c_2$  are the wave velocities of the respective materials. In the following, all quantities such as the elastic constants, stresses, and so on, pertaining to the material 1 and material 2 will be marked with subscript 1 and 2, respectively. Initial conditions are

$$\begin{aligned}
 u_i(x,0) &= 0 \\
 \frac{\partial}{\partial t} u_i(x,0) &= 0 \quad i=1,2
 \end{aligned}
 \tag{6}$$

Applying the Laplace transform over t to the governing equations gives

$$\begin{aligned}
 V_1 &= \frac{1}{c_1^2} p^2 V_1 \\
 V_2 &= \frac{1}{c_2^2} p^2 V_2
 \end{aligned}
 \tag{7}$$

where

$$V_i(x,p) = \mathcal{L}[u_i(x,t)] = \int_0^{\infty} u_i(x,t) e^{-pt} dt$$

and

$$V_i(x,p) = \frac{\partial^2}{\partial x^2} V_i(x,p) \quad i=1,2$$

Seeking the solutions, we write directly

$$\begin{aligned}
V_1(x,p) &= Ae^{\frac{p}{c_1}x} + Be^{-\frac{p}{c_1}x} \\
V_2(x,p) &= Ce^{\frac{p}{c_2}x} + De^{-\frac{p}{c_2}x}
\end{aligned}
\tag{8}$$

where A, B, C and D are the coefficients to be determined from the boundary conditions. The boundary conditions for the problem are given as

$$\begin{aligned}
\text{a. } & x = h_2, \quad \sigma_2 = 0 \\
\text{b. } & x = 0, \quad \sigma_1 = \sigma_2, \quad u_1 = u_2 \\
\text{c. } & x = -h_1, \quad \sigma_1 = f(t)
\end{aligned}
\tag{9}$$

Boundary conditions a and c are obvious because right side of the material 2 is stress-free and left side of the material 1 is where the initial stress pulse is applied. The shape of initial stress pulse is not decided yet. The conditions at  $x=0$  express continuity of displacement and force at the interface of two materials. Applying the Laplace transform to the boundary conditions gives

$$\begin{aligned}
x = h_2 & \quad E_2 \frac{\partial}{\partial x} V_2 = 0 \\
x = 0 & \quad E_1 \frac{\partial}{\partial x} V_1 = E_2 \frac{\partial}{\partial x} V_2, \quad V_1 = V_2 \\
x = -h_1 & \quad E_1 \frac{\partial}{\partial x} V_1 = \bar{f}(p)
\end{aligned}
\tag{10}$$

where  $\bar{f}(p)$  is the incident stress pulse transformed

Applying these transformed conditions to the solutions (7) gives the following four linear equations in A, B, C, and D.

$$\begin{aligned}
 C - e^{\frac{2ph_2}{c_2}} D &= 0 \\
 A - B - \frac{c_1 E_2}{c_2 E_1} (C - D) &= 0 \\
 A + B - C - D &= 0 \\
 A - e^{\frac{2ph_1}{c_1}} B &= -\frac{c_1}{E_1 p} e^{\frac{ph_1}{c_1}} \bar{f}(p)
 \end{aligned} \tag{11}$$

Solving these linear equations gives expressions for the four coefficients as

$$\begin{aligned}
A &= \frac{\frac{c_1}{E_1 p} e^{\frac{ph_1}{c_1}} \bar{f}(p) \left[ \left(1 + \frac{c_1 E_2}{c_2 E_1}\right) e^{\frac{2ph_2}{c_2}} + \left(1 - \frac{c_1 E_2}{c_2 E_1}\right) \right]}{\left(1 - \frac{c_1 E_2}{c_2 E_1}\right) \left(e^{\frac{2ph_1}{c_1}} e^{\frac{2ph_2}{c_2}} - 1\right) + \left(1 + \frac{c_1 E_2}{c_2 E_1}\right) \left(e^{\frac{2ph_1}{c_1}} - e^{\frac{2ph_2}{c_2}}\right)} \\
B &= \frac{\frac{c_1}{E_1 p} e^{\frac{ph_1}{c_1}} \bar{f}(p) \left[ \left(1 - \frac{c_1 E_2}{c_2 E_1}\right) e^{\frac{2ph_2}{c_2}} + \left(1 + \frac{c_1 E_2}{c_2 E_1}\right) \right]}{\left(1 - \frac{c_1 E_2}{c_2 E_1}\right) \left(e^{\frac{2ph_1}{c_1}} e^{\frac{2ph_2}{c_2}} - 1\right) + \left(1 + \frac{c_1 E_2}{c_2 E_1}\right) \left(e^{\frac{2ph_1}{c_1}} - e^{\frac{2ph_2}{c_2}}\right)} \\
C &= \frac{\frac{2c_1}{E_1 p} e^{\frac{ph_1}{c_1}} e^{\frac{2ph_2}{c_2}} \bar{f}(p)}{\left(1 - \frac{c_1 E_2}{c_2 E_1}\right) \left(e^{\frac{2ph_1}{c_1}} e^{\frac{2ph_2}{c_2}} - 1\right) + \left(1 + \frac{c_1 E_2}{c_2 E_1}\right) \left(e^{\frac{2ph_1}{c_1}} - e^{\frac{2ph_2}{c_2}}\right)} \\
D &= \frac{\frac{2c_1}{E_1 p} e^{\frac{ph_1}{c_1}} \bar{f}(p)}{\left(1 - \frac{c_1 E_2}{c_2 E_1}\right) \left(e^{\frac{2ph_1}{c_1}} e^{\frac{2ph_2}{c_2}} - 1\right) + \left(1 + \frac{c_1 E_2}{c_2 E_1}\right) \left(e^{\frac{2ph_1}{c_1}} - e^{\frac{2ph_2}{c_2}}\right)}
\end{aligned} \tag{12}$$

After some algebraic manipulations we express coefficients A, B, C and D as

$$\begin{aligned}
A &= - \frac{\frac{c_1}{E_1 p} \bar{f}(p) e^{\frac{ph_1}{c_1}} (1 + \lambda e^{\frac{2ph_2}{c_2}})}{1 - \epsilon} \\
B &= - \frac{\frac{c_1}{E_1 p} \bar{f}(p) e^{\frac{ph_1}{c_1}} (\lambda + e^{\frac{2ph_2}{c_2}})}{1 - \epsilon} \\
C &= - \frac{\frac{2c_1 c_2}{c_1 E_2 + c_2 E_1} \frac{1}{p} \bar{f}(p) e^{\frac{ph_1}{c_1}}}{1 - \epsilon} \\
D &= - \frac{\frac{2c_1 c_2}{c_1 E_2 + c_2 E_1} \frac{1}{p} \bar{f}(p) e^{\frac{ph_1}{c_1}} e^{\frac{2ph_2}{c_2}}}{1 - \epsilon}
\end{aligned} \tag{13}$$

where the constants  $\lambda$  and  $\epsilon$  are defined by

$$\begin{aligned}
\lambda &= \frac{c_2 E_1 - c_1 E_2}{c_2 E_1 + c_1 E_2} \\
\epsilon &= \frac{c_2 E_1 - c_1 E_2}{c_2 E_1 + c_1 E_2} (e^{\frac{2ph_1}{c_1}} - e^{\frac{2ph_2}{c_2}}) + e^{\frac{2ph_1}{c_1}} e^{\frac{2ph_2}{c_2}}
\end{aligned}$$

Now we need to decide the shape of incident stress pulse. If a rectangular shaped stress pulse is taken to be the incident pulse, the expression for this stress pulse is

$$f(t) = -\sigma_0[H(t) - H(t-t_0)] \quad (14)$$

where H is the Heaviside step function,

'-' sign means that the stress is compressive,

$\sigma_0$  is the magnitude of the stress pulse applied and

$t_0$  is the time-duration for the initial stress pulse applied.

Applying the Laplace transform over t to the incident stress pulse expression gives

$$\bar{f}(p) = -\frac{\sigma_0}{p}(1 - e^{-pt_0}) \quad (15)$$

If we rewrite the expression  $1/(1-\epsilon)$  in the form of infinite series

$$\frac{1}{1 - \epsilon} = \sum_{n=0}^{\infty} \epsilon^n \quad |\epsilon| < 1 \quad (16)$$

substituting the expressions (14) and (15) in (12) gives

$$\begin{aligned}
A &= \frac{c_1 \sigma_0}{E_1} \frac{1}{p^2} \sum_{n=0}^{\infty} \epsilon^n \left[ e^{-p \left( \frac{h_1}{c_1} \right)} + \lambda e^{-p \left( \frac{h_1}{c_1} + 2 \frac{h_2}{c_2} \right)} - e^{-p \left( t_0 + \frac{h_1}{c_1} \right)} - \lambda e^{-p \left( t_0 + \frac{h_1}{c_1} + 2 \frac{h_2}{c_2} \right)} \right] \\
B &= \frac{c_1 \sigma_0}{E_1} \frac{1}{p^2} \sum_{n=0}^{\infty} \epsilon^n \left[ \lambda e^{-p \left( \frac{h_1}{c_1} \right)} + e^{-p \left( \frac{h_1}{c_1} + 2 \frac{h_2}{c_2} \right)} - \lambda e^{-p \left( t_0 + \frac{h_1}{c_1} \right)} - e^{-p \left( t_0 + \frac{h_1}{c_1} + 2 \frac{h_2}{c_2} \right)} \right] \\
C &= \frac{2c_1 c_2 \sigma_0}{c_1 E_2 + c_2 E_1} \frac{1}{p^2} \sum_{n=0}^{\infty} \epsilon^n \left[ e^{-p \left( \frac{h_1}{c_1} \right)} - e^{-p \left( t_0 + \frac{h_1}{c_1} \right)} \right] \\
D &= \frac{2c_1 c_2 \sigma_0}{c_1 E_2 + c_2 E_1} \frac{1}{p^2} \sum_{n=0}^{\infty} \epsilon^n \left[ e^{-p \left( \frac{h_1}{c_1} + 2 \frac{h_2}{c_2} \right)} - e^{-p \left( t_0 + \frac{h_1}{c_1} + 2 \frac{h_2}{c_2} \right)} \right]
\end{aligned} \tag{17}$$

The complete expressions for  $V_1$  and  $V_2$  then become

$$\begin{aligned}
V_1(x,p) &= A e^{-\frac{p x}{c_1}} + B e^{\frac{p x}{c_1}} \\
&= \frac{c_1 \sigma_0}{E_1} \frac{1}{p^2} \sum_{n=0}^{\infty} \epsilon^n \left\{ \lambda \left[ e^{-p \left( \frac{h_1}{c_1} + 2 \frac{h_2}{c_2} + \frac{x}{c_1} \right)} - e^{-p \left( t_0 + \frac{h_1}{c_1} + 2 \frac{h_2}{c_2} + \frac{x}{c_1} \right)} \right] \right. \\
&\quad + \left. e^{-p \left( \frac{h_1}{c_1} - \frac{x}{c_1} \right)} - e^{-p \left( t_0 + \frac{h_1}{c_1} - \frac{x}{c_1} \right)} \right] \\
&\quad + \left. e^{-p \left( \frac{h_1}{c_1} + \frac{x}{c_1} \right)} - e^{-p \left( t_0 + \frac{h_1}{c_1} + \frac{x}{c_1} \right)} + e^{-p \left( \frac{h_1}{c_1} + 2 \frac{h_2}{c_2} - \frac{x}{c_1} \right)} - e^{-p \left( t_0 + \frac{h_1}{c_1} + 2 \frac{h_2}{c_2} - \frac{x}{c_1} \right)} \right\}
\end{aligned} \tag{18}$$

$$\begin{aligned}
V_2(x,p) &= \frac{2c_1 c_2 \sigma_0}{c_1 E_2 + c_2 E_1} \frac{1}{p^2} \sum_{n=0}^{\infty} \epsilon^n \left\{ \left[ e^{-p \left( \frac{h_1}{c_1} + \frac{x}{c_2} \right)} + e^{-p \left( \frac{h_1}{c_1} + 2 \frac{h_2}{c_2} - \frac{x}{c_2} \right)} \right] \right. \\
&\quad \left. - e^{-p \left( t_0 + \frac{h_1}{c_1} + \frac{x}{c_2} \right)} - e^{-p \left( t_0 + \frac{h_1}{c_1} + 2 \frac{h_2}{c_2} - \frac{x}{c_2} \right)} \right\}
\end{aligned} \tag{19}$$



The final stress expressions are obtained by using the relation

$$\sigma_i = E_i \frac{\partial u_i}{\partial x} = E_i \mathcal{L}^{-1} \left( \frac{\partial}{\partial x} V_i \right) \quad (20)$$

where  $\mathcal{L}^{-1}$  is the inverse Laplace transform and  $i = 1, 2$ .

Thus,

$$\begin{aligned} \sigma_1(x,t) = \sigma_0 \mathcal{L}^{-1} \left\{ \frac{1}{p} \sum_{n=0}^{\infty} \epsilon^n \left\{ \lambda \left[ - e^{-p \left( \frac{h_1}{c_1} + 2 \frac{h_2}{c_2} + \frac{x}{c_1} \right)} + e^{-p \left( t_0 + \frac{h_1}{c_1} + 2 \frac{h_2}{c_2} + \frac{x}{c_1} \right)} \right. \right. \right. \\ \left. \left. + e^{-p \left( \frac{h_1}{c_1} - \frac{x}{c_1} \right)} - e^{-p \left( t_0 + \frac{h_1}{c_1} - \frac{x}{c_1} \right)} \right] \right. \\ \left. - e^{-p \left( \frac{h_1}{c_1} + \frac{x}{c_1} \right)} + e^{-p \left( t_0 + \frac{h_1}{c_1} + \frac{x}{c_1} \right)} \right. \\ \left. + e^{-p \left( \frac{h_1}{c_1} + 2 \frac{h_2}{c_2} - \frac{x}{c_1} \right)} - e^{-p \left( t_0 + \frac{h_1}{c_1} + 2 \frac{h_2}{c_2} - \frac{x}{c_1} \right)} \right\} \right\} \quad (21) \end{aligned}$$

$$\begin{aligned} \sigma_2(x,t) = \frac{2c_1 E_2 \sigma_0}{c_1 E_2 + c_2 E_1} \mathcal{L}^{-1} \left\{ \frac{1}{p} \sum_{n=0}^{\infty} \epsilon^n \left[ - e^{-p \left( \frac{h_1}{c_1} + \frac{x}{c_2} \right)} + e^{-p \left( \frac{h_1}{c_1} + 2 \frac{h_2}{c_2} - \frac{x}{c_2} \right)} \right. \right. \\ \left. \left. + e^{-p \left( t_0 + \frac{h_1}{c_1} + \frac{x}{c_2} \right)} - e^{-p \left( t_0 + \frac{h_1}{c_1} + 2 \frac{h_2}{c_2} - \frac{x}{c_2} \right)} \right] \right\} \quad (22) \end{aligned}$$

Now we have two stress expressions for  $\sigma_1$  and  $\sigma_2$ . If these two expressions are correct, by the continuity at the interface,  $\sigma_1$  has to be equal to  $\sigma_2$  when

$x=0$ .

$$\sigma_1(0,t) = \sigma_0 (1 - \lambda) \mathcal{L}^{-1} \left\{ \frac{1}{p} \sum_{n=0}^{\infty} \epsilon^n \left[ e^{-p\left(\frac{h_1}{c_1} + 2\frac{h_2}{c_2}\right)} - e^{-p\left(t_0 + \frac{h_1}{c_1} + 2\frac{h_2}{c_2}\right)} - e^{-p\left(\frac{h_1}{c_1}\right)} + e^{-p\left(t_0 + \frac{h_1}{c_1}\right)} \right] \right\} \quad (23)$$

$$\sigma_2(0,t) = \frac{2c_1E_2\sigma_0}{c_1E_2 + c_2E_1} \mathcal{L}^{-1} \left\{ \frac{1}{p} \sum_{n=0}^{\infty} \epsilon^n \left[ e^{-p\left(\frac{h_1}{c_1} + 2\frac{h_2}{c_2}\right)} - e^{-p\left(t_0 + \frac{h_1}{c_1} + 2\frac{h_2}{c_2}\right)} - e^{-p\left(\frac{h_1}{c_1}\right)} + e^{-p\left(t_0 + \frac{h_1}{c_1}\right)} \right] \right\} \quad (24)$$

$$1 - \lambda = 1 - \frac{c_2E_1 - c_1E_2}{c_2E_1 + c_1E_2} = \frac{2c_1E_2}{c_1E_2 + c_2E_1} \quad (25)$$

By (22) and (23), we see that the continuity condition at the interface is satisfied.

### 3. Results and Discussion

The computations to obtain  $\sigma_1^*$  and  $\sigma_2$  are done by the Maple programming summarized in the following.

$$\begin{aligned}
 \text{Step 1} &= \frac{\partial}{\partial x} V_1 && \left( \frac{\partial}{\partial x} V_2 \text{ for } \sigma_2 \right) \\
 \text{Step 2} &= \mathcal{L}^{-1} \left( \frac{\partial}{\partial x} V_1 \right) \\
 &= \mathcal{L}^{-1}(\text{Step 1}) && \left( \mathcal{L}^{-1} \left( \frac{\partial}{\partial x} V_2 \right) \text{ for } \sigma_2 \right) \\
 \text{Step 3} &= E_1 \mathcal{L}^{-1} \left( \frac{\partial}{\partial x} V_1 \right) && (26) \\
 &= E_1 \text{Step 2} && \left( E_2 \mathcal{L}^{-1} \left( \frac{\partial}{\partial x} V_2 \right) \text{ for } \sigma_2 \right) \\
 \text{Step 4} &= \textit{Substitution of material properties such as } E_1, E_2, c_1, c_2, \\
 &\quad \textit{demensions } h_1, h_2, \textit{ magnitude of initial incident stress pulse } \sigma_0, \\
 &\quad \textit{time duration } t_0 \textit{ into Step 3} \\
 \text{Step 5} &= \textit{Plotting Step 4**}
 \end{aligned}$$

As shown above, the program includes the calculation of infinite series.

\* Hereafter only  $\sigma_1$  is focused on because as stated in the introduction, the goal of this study is the analysis of stress-state at the interface, and only one stress expression, either  $\sigma_1$  or  $\sigma_2$  is required for it. But the expression of  $\sigma_2$  is mentioned in order to explain the concept of impedance.

\*\* When plotting, substitution of  $x=0$  (location of the interface) in Step 4 has to be made first to obtain a plot for  $\sigma_1(0,t)$  and  $\sigma_2(0,t)$ .

So the accuracy of the final result depends on how accurate the infinite series calculation is. The more terms we take, the better result we obtain.

However, due to the limited capability of computer, we cannot and need not take infinite number of terms for the calculation of maximum interface stress.

In most cases, not so many terms are required because stress pulse large enough to cause a failure can be developed by the interference of reflected pulses at the interface before such a long time passes on. Also note that since the solution is given as the sum of step functions, the truncated series gives the exact solution up to a certain value of time.

Before proceeding to the analysis of stress-state for specific cases, we examine a simple general case of this problem for better understanding the physical meaning of the each terms in the stress expression. For simplicity consider the case of  $n=0$ .

Thus  $\sigma_1$  at  $x=0$  becomes

$$\begin{aligned}
\sigma_1(0,t) = & - \sigma_0 \left[ \lambda H\left(t - \frac{h_1}{c_1} - 2\frac{h_2}{c_2}\right) - \lambda H\left(t - t_0 - \frac{h_1}{c_1} - 2\frac{h_2}{c_2}\right) \right. \\
& - \lambda H\left(t - \frac{h_1}{c_1}\right) + \lambda H\left(t - t_0 - \frac{h_1}{c_1}\right) \\
& + H\left(t - \frac{h_1}{c_1}\right) - H\left(t - t_0 - \frac{h_1}{c_1}\right) \\
& \left. - H\left(t - \frac{h_1}{c_1} - 2\frac{h_2}{c_2}\right) + H\left(t - t_0 - \frac{h_1}{c_1} - 2\frac{h_2}{c_2}\right) \right] \quad (27)
\end{aligned}$$

Note that in (27), every pair of two terms in the same row makes one complete rectangular-shaped stress pulse with time duration  $t_0$ . Hereafter those two terms in the same row will be called "pair". Recalling that the initial compressive stress applied has the form of

$$f(t) = - \sigma_0 [H(t) - H(t - t_0)]$$



we instantly observe that third pair is simply the initial compressive stress pulse propagated to the interface.  $h_1/c_1$  is the time spent for the stress pulse to reach the interface from the end where the initial stress pulse is applied.

Also, the second pair is a stress pulse acting on the interface at the same time. Although the time at which both stress pulses act is same, their physical meaning is far different. To get the clear understanding, the stress expression before substituting  $x=0$  in Step 3 is reviewed.

$$\begin{aligned}
\sigma_1(x,t) = & - \sigma_0 \left[ \lambda H\left(t - \frac{h_1}{c_1} - 2\frac{h_2}{c_2} - \frac{x}{c_1}\right) - \lambda H\left(t - t_0 - \frac{h_1}{c_1} - 2\frac{h_2}{c_2} - \frac{x}{c_1}\right) \right. \\
& - \lambda H\left(t - \frac{h_1}{c_1} + \frac{x}{c_1}\right) + \lambda\left(t - t_0 - \frac{h_1}{c_1} + \frac{x}{c_1}\right) \\
& + H\left(t - \frac{h_1}{c_1} - \frac{x}{c_1}\right) - H\left(t - t_0 - \frac{h_1}{c_1} - \frac{x}{c_1}\right) \\
& \left. + H\left(t - \frac{h_1}{c_1} - 2\frac{h_2}{c_2} + \frac{x}{c_1}\right) + H\left(t - t_0 - \frac{h_1}{c_1} - 2\frac{h_2}{c_2} + \frac{x}{c_1}\right) \right] \quad (28)
\end{aligned}$$

If we substitute a number which is very close to zero ( which is a negative number since we are considering the stress-state expressed in terms of  $\sigma_1$  ), such as  $-\Delta x$ , in  $x$ , for the time  $h_1/c_1 - \Delta x/c_1$ , the incident stress pulse traveling along the material 1 reaches somewhere very close to the interface, but it has not reached the interface yet. On the other hand, for the time  $h_1/c_1 + \Delta x/c_1$ , the incident stress pulse returns toward the left end of the rod after finishing interaction at the interface. In other words, the physical meaning of the third pair is the incident stress pulse just before the interaction and the second pair is the reflected stress pulse right after the interaction. If we continuously keep decreasing the absolute value of  $x$  until  $x$  equals to exact 0, the incident stress pulse and the reflected stress pulse superpose without time-delay, that is, incidence and reflection of the stress pulse occur simultaneously. One more thing that should be mentioned here is the role of

$\lambda$  in the stress expression. The multiplier  $\lambda$  plays a role as impedance of which the term and concept is borrowed from electric circuit theory. Here, it gives a change to the magnitude of incident stress pulse when reflected from the interface. As obtained in the previous study, the expression for  $\lambda$  is given by

$$\lambda = \frac{c_2 E_1 - c_1 E_2}{c_2 E_1 + c_1 E_2} \quad (29)$$

The multiplier  $\lambda$  not only influence on the magnitude of the incident stress pulse, but also may change its sign. If  $c_2 E_1 - c_1 E_2 < 0$ , the incident stress pulse is reflected with change only in its magnitude, but if  $c_2 E_1 - c_1 E_2 > 0$ , it is reflected with changed sign as well as magnitude, that is, reflected stress pulse is tensile when incidence was compressive, and vice versa. If we examine the time domains of the Heaviside functions of the first and fourth pair in (27), we can easily see that these are two stress pulses transmitted through the interface. For the time  $h_1/c_1 + 2h_2/c_2$ , they are transmitted from material 1 into material 2, propagated toward the right side free end, and returned to the interface. Each stress transmission is produced by the incident

and reflected stress pulse, that is, the first pair is produced by the second pair, the fourth pair by the third. Hence, the first pair has the same magnitude as the second and the fourth as the third. Note that the sign of the first and the fourth pairs are opposite to the second and the third pairs though they should have the same signs by the continuity at the interface when transmission occurs. The reason is quite simple. The first and the fourth pairs are the ones experienced the reflection at the right side free end, thus they had changes in their signs when reflected. The stress reversal is a characteristic of free end condition.

All the analyses above satisfy the validity by the stress continuity at the interface, that is,

$$\sigma_i + \sigma_r = \sigma_t \quad (30)$$

where  $\sigma_i$  is incident stress

$\sigma_r$  is reflected stress

$\sigma_t$  is transmitted stress

Suppose that we have an incident stress pulse expressed by

$$\sigma_i = -\sigma_0 \left[ H\left(t - \frac{h_1}{c_1}\right) - H\left(t - t_0 - \frac{h_1}{c_1}\right) \right] \quad (31)$$



Then, simultaneously, we have a reflected stress pulse and a transmitted stress pulse expressed by

$$\begin{aligned}
 \sigma_r &= -\sigma_0 \left[ -\lambda H\left(t - \frac{h_1}{c_1}\right) + \lambda H\left(t - t_0 - \frac{h_1}{c_1}\right) \right] \\
 \sigma_t &= -\sigma_0 \left[ H\left(t - \frac{h_1}{c_1}\right) - H\left(t - t_0 - \frac{h_1}{c_1}\right) \right] \\
 &\quad - \sigma_0 \left[ -\lambda H\left(t - \frac{h_1}{c_1}\right) + \lambda H\left(t - t_0 - \frac{h_1}{c_1}\right) \right] \\
 &= -\sigma_0 (1 - \lambda) \left[ H\left(t - \frac{h_1}{c_1}\right) - H\left(t - t_0 - \frac{h_1}{c_1}\right) \right]
 \end{aligned} \tag{32}$$

This situation is same as (27) except that the transmitted stress pulse is just produced, and has not experienced reflection at the free end yet. From (31) and (32), we see that (30) is satisfied.

In (32),  $\sigma_t$  is given in terms of the multiplier for reflection,  $\lambda$ . We can express  $\sigma_t$  in terms of the multiplier for transmission,  $\mu$ . At the interface ( $x=0, \sigma_1=\sigma_2$ ),  $\sigma_2$  (when  $n=0$ ) is given by

$$\begin{aligned}
 \sigma_2 &= -\sigma_0 \left[ \mu H\left(t - \frac{h_1}{c_1}\right) - \mu H\left(t - t_0 - \frac{h_1}{c_1}\right) \right. \\
 &\quad \left. - \mu H\left(t - \frac{h_1}{c_1} - 2\frac{h_2}{c_2}\right) + \mu H\left(t - t_0 - \frac{h_1}{c_1} - 2\frac{h_2}{c_2}\right) \right]
 \end{aligned} \tag{33}$$

where

$$\mu = \frac{2c_1E_2}{c_1E_2 + c_2E_1}$$

Examining the time domains in (33), we instantly know the first pair is the stress pulse just transmitted from material 1 and the second pair is the transmitted stress pulse after reflection from the free end. Thus, the first pair in (33) should equal to  $\sigma_t$  in (32).

$$\begin{aligned} \text{The first pair of (33)} &= -\sigma_0 \left[ \mu H\left(t - \frac{h_1}{c_1}\right) - \mu H\left(t - t_0 - \frac{h_1}{c_1}\right) \right] \\ &= -\sigma_0 \frac{2c_1E_2}{c_1E_2 + c_2E_1} \left[ H\left(t - \frac{h_1}{c_1}\right) - H\left(t - t_0 - \frac{h_1}{c_1}\right) \right] \\ \sigma_t \text{ of (32)} &= -\sigma_0 (1 - \lambda) \left[ H\left(t - \frac{h_1}{c_1}\right) - H\left(t - t_0 - \frac{h_1}{c_1}\right) \right] \\ &= -\sigma_0 \left( 1 - \frac{c_2E_1 - c_1E_2}{c_2E_1 + c_1E_2} \right) \left[ H\left(t - \frac{h_1}{c_1}\right) - H\left(t - t_0 - \frac{h_1}{c_1}\right) \right] \\ &= -\sigma_0 \frac{2c_1E_2}{c_1E_2 + c_2E_1} \left[ H\left(t - \frac{h_1}{c_1}\right) - H\left(t - t_0 - \frac{h_1}{c_1}\right) \right] \end{aligned}$$

The multiplier  $\mu$  plays the same role as  $\lambda$ . It gives a change to the magnitude of incident stress pulse when transmitted through the interface but it does not change the sign of incident stress pulse. Hence, if we use  $\lambda$  and  $\mu$ , we can express the reflected and transmitted stress pulses in simple forms

given by

$$\begin{aligned}\sigma_t &= \mu \sigma_i = \frac{2c_1 E_2}{c_1 E_2 + c_2 E_1} \sigma_i \\ \sigma_r &= -\lambda \sigma_i = -\frac{c_2 E_1 - c_1 E_2}{c_2 E_1 + c_1 E_2} \sigma_i\end{aligned}\tag{34}$$

So far, we analysed all the stress wave behaviors produced when  $n=0$  is substituted in the final solution (21). If we extend our study to the case of  $n=1$ , we have a more complicated form of stress expression given by (35). Each group of stress pulses represents one complete stress pulse acting on the interface. As shown in Fig. 3, one stress pulse initially applied leads to quite complicated stress distribution. Of course, if we substitute  $n=3,4,-----$ , transmission occurs at 2, transmission and reflection at 3, reflection at 4, transmission at 5, transmission and reflection at 6, and many other points where transmission or reflection or both occur will appear on the interface.

$$\begin{aligned}
\sigma_1(0,t) = & -\sigma_0 \left[ H\left(t - \frac{h_1}{c_1}\right) - H\left(t - t_0 - \frac{h_1}{c_1}\right) \right. \\
& - \lambda H\left(t - \frac{h_1}{c_1}\right) + \lambda H\left(t - t_0 - \frac{h_1}{c_1}\right) \quad \Rightarrow \text{GROUP 1} \\
& - H\left(t - \frac{h_1}{c_1} - 2\frac{h_2}{c_2}\right) + H\left(t - t_0 - \frac{h_1}{c_1} - 2\frac{h_2}{c_2}\right) \\
& + \lambda^2 H\left(t - \frac{h_1}{c_1} - 2\frac{h_2}{c_2}\right) - \lambda^2 H\left(t - t_0 - \frac{h_1}{c_1} - 2\frac{h_2}{c_2}\right) \quad \Rightarrow \text{GROUP 2} \\
& + \lambda H\left(t - \frac{h_1}{c_1} - 4\frac{h_2}{c_2}\right) - \lambda H\left(t - t_0 - \frac{h_1}{c_1} - 4\frac{h_2}{c_2}\right) \\
& - \lambda^2 H\left(t - \frac{h_1}{c_1} - 4\frac{h_2}{c_2}\right) + \lambda^2 H\left(t - t_0 - \frac{h_1}{c_1} - 4\frac{h_2}{c_2}\right) \quad \Rightarrow \text{GROUP 3} \\
& + \lambda H\left(t - 3\frac{h_1}{c_1}\right) - \lambda H\left(t - t_0 - 3\frac{h_1}{c_1}\right) \\
& - \lambda^2 H\left(t - 3\frac{h_1}{c_1}\right) + \lambda^2 H\left(t - t_0 - 3\frac{h_1}{c_1}\right) \quad \Rightarrow \text{GROUP 4} \\
& + H\left(t - 3\frac{h_1}{c_1} - 2\frac{h_2}{c_2}\right) - H\left(t - t_0 - 3\frac{h_1}{c_1} - 2\frac{h_2}{c_2}\right) + \lambda^2 H\left(t - 3\frac{h_1}{c_1} - 2\frac{h_2}{c_2}\right) - \lambda^2 H\left(t - t_0 - 3\frac{h_1}{c_1} - 2\frac{h_2}{c_2}\right) \\
& - 2\lambda H\left(t - 3\frac{h_1}{c_1} - 2\frac{h_2}{c_2}\right) + 2\lambda H\left(t - t_0 - 3\frac{h_1}{c_1} - 2\frac{h_2}{c_2}\right) \quad \Rightarrow \text{GROUP 5} \\
& - H\left(t - 3\frac{h_1}{c_1} - 4\frac{h_2}{c_2}\right) + H\left(t - t_0 - 3\frac{h_1}{c_1} - 4\frac{h_2}{c_2}\right) \\
& \left. + \lambda H\left(t - 3\frac{h_1}{c_1} - 4\frac{h_2}{c_2}\right) - \lambda H\left(t - t_0 - 3\frac{h_1}{c_1} - 4\frac{h_2}{c_2}\right) \right] \quad \Rightarrow \text{GROUP 6}
\end{aligned} \tag{35}$$

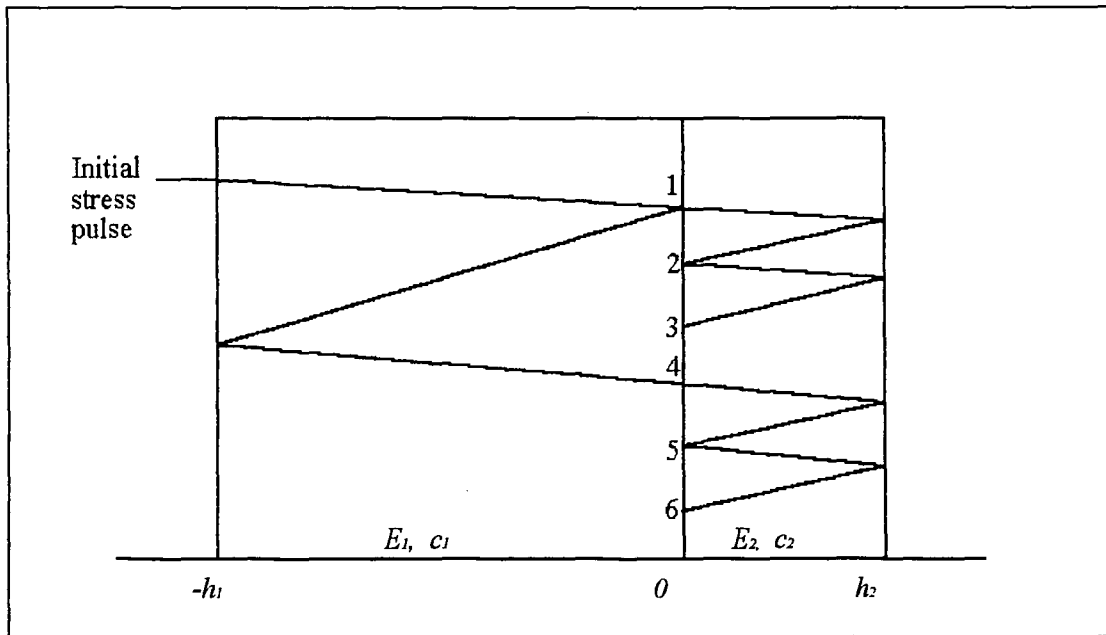


Fig.3 Stress wave behaviors in a two-part composite rod( $n=1$ )

One more thing noteworthy is that when  $n=1$  is substituted, there is a reflection at 2 which makes a change of magnitude of stress pulse, compared to the case when  $n=0$  is substituted. To visualize this phenomenon, plots are made by giving real values of existing material properties to the program we already have. For the case of copper and brass bonding, the material properties are included in Table 1.

	E(psi)	$\rho$ (lb/in <sup>3</sup> )	c(in/sec)	h(inch)
Material 1(Brass*)	$15 \times 10^6$	0.304	138030.7	1.5
Material 2(Copper*)	$17.5 \times 10^6$	0.324	144415.3	0.5

Table 1. Elastic constants of Brass and Copper

To observe the results clearly we assume that initial stress pulse with magnitude 1 psi is applied for  $10^{-6}$  second, and the lengths of the material 1 and material 2 are 1.5 inch and 0.5 inch, respectively. Two plots for  $n=0$  and  $n=1$  are presented in the following(Fig.4 and 5). As seen in Fig. 5, magnitude of the first tensile stress pulse is decreased by the reflection that occurs at 2. According to this phenomenon, we can expect that more changes will exist if a transmission occurs at 2. Similarly, there exist many more complicated stress pulse interferences as time goes by. Sometimes two or more stress pulses may be superposed to double up the magnitude, or two opposite pulses may be canceled out, and so on. Fig.6 shows the stress distribution on the interface when  $n=5$ .

\*From reference [14]

By using the program we have made, we can obtain stress distribution at any location other than interface in the rod. Fig.7 shows the stress distribution at  $x=0.25$  inch( middle of material 2 ).

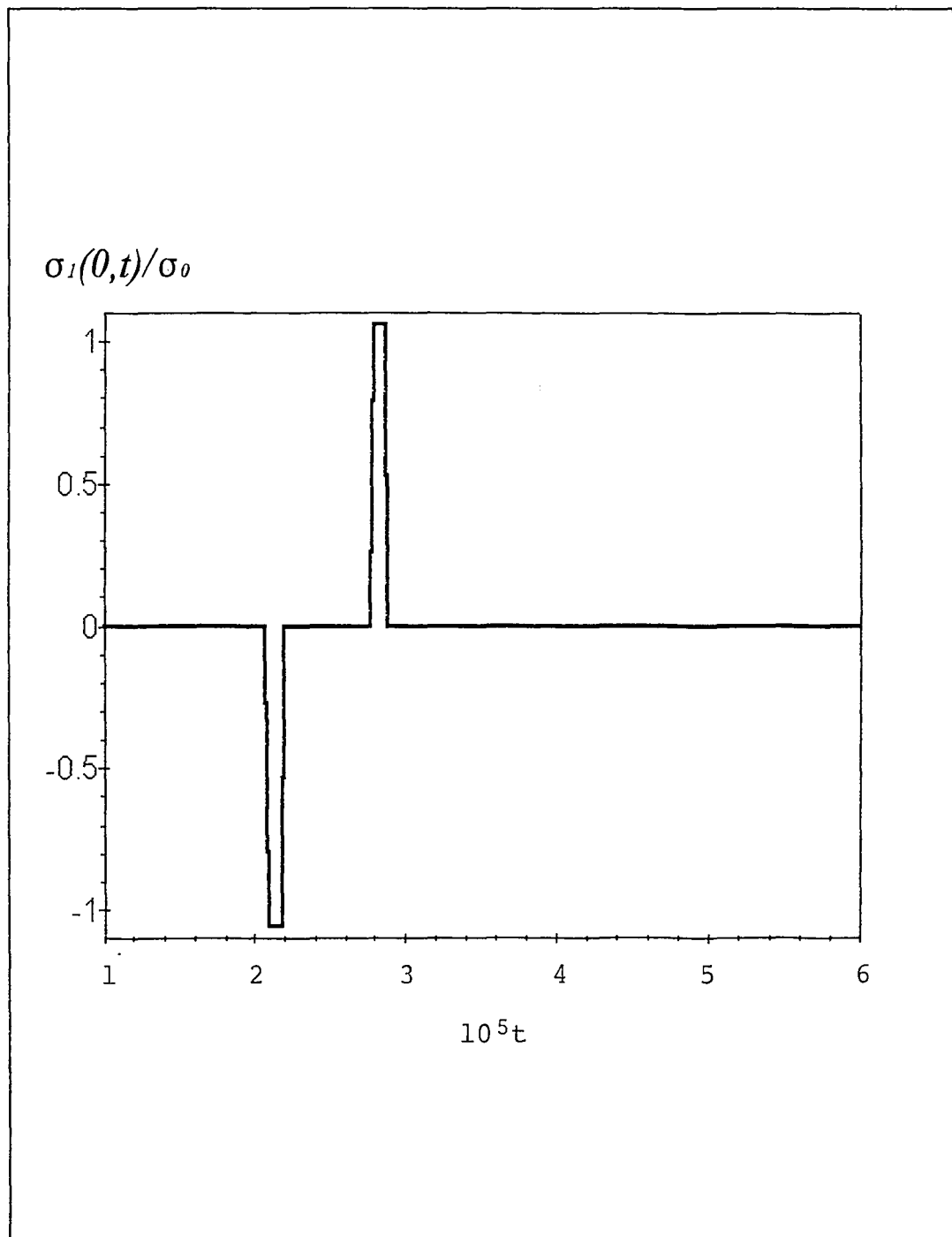


Fig.4 Stress distribution on the interface(Materials: 1 Brass,  
2 Copper, n=0)



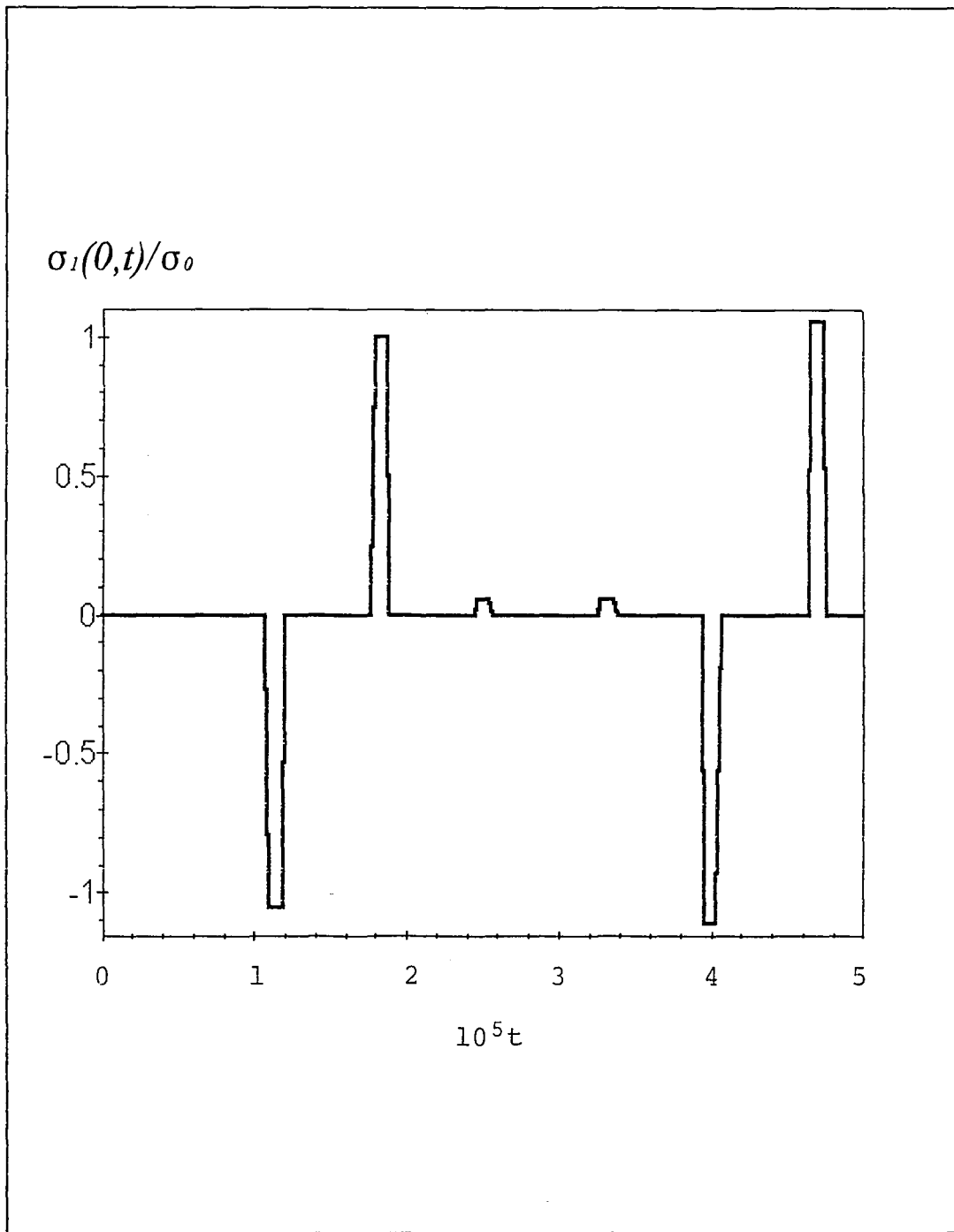


Fig.5 Stress distribution on the interface(Materials: 1 Brass,  
2 Copper, n=1)

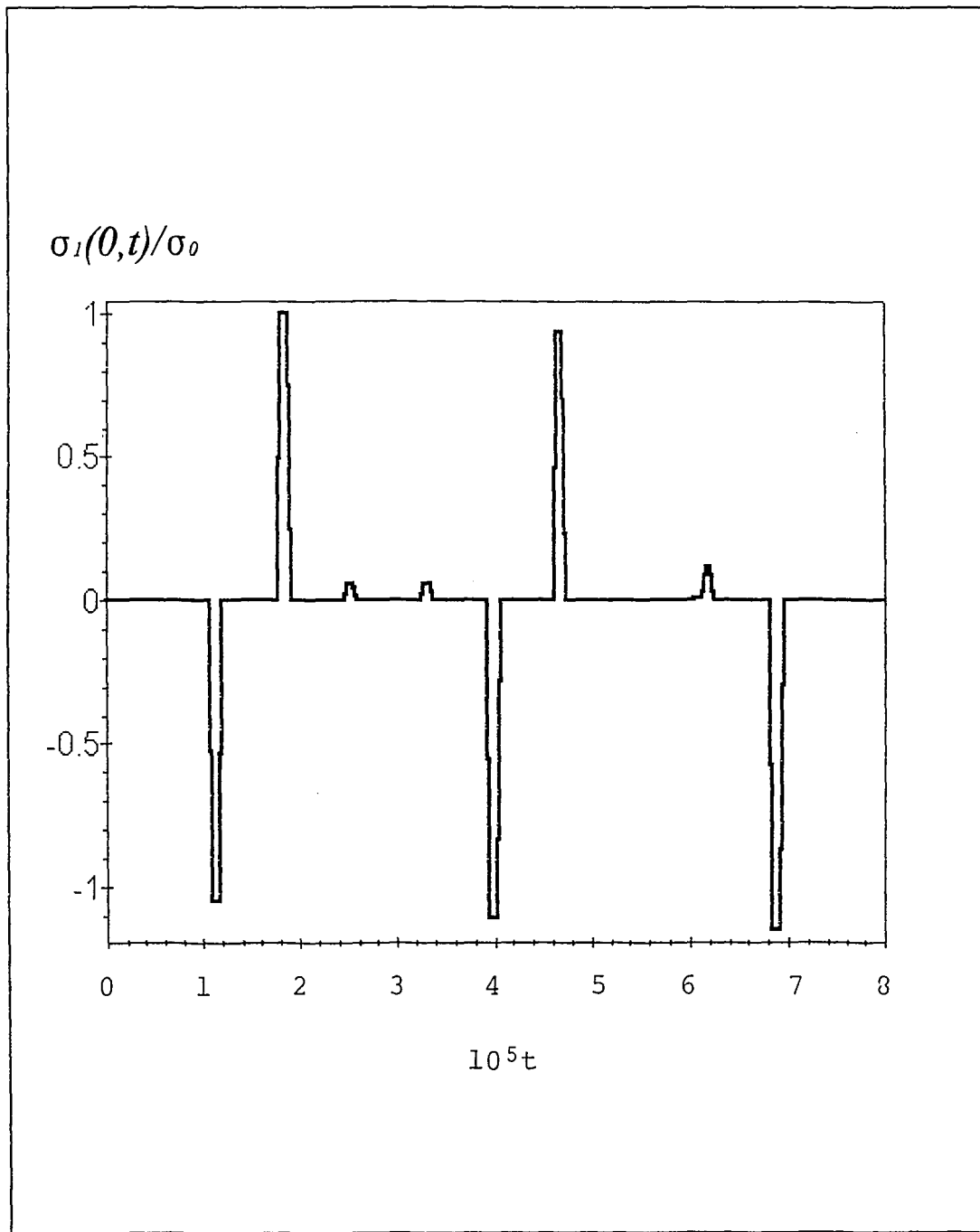


Fig.6 Stress distribution on the interface(Materials: 1 Brass,  
2 Copper, n=5)

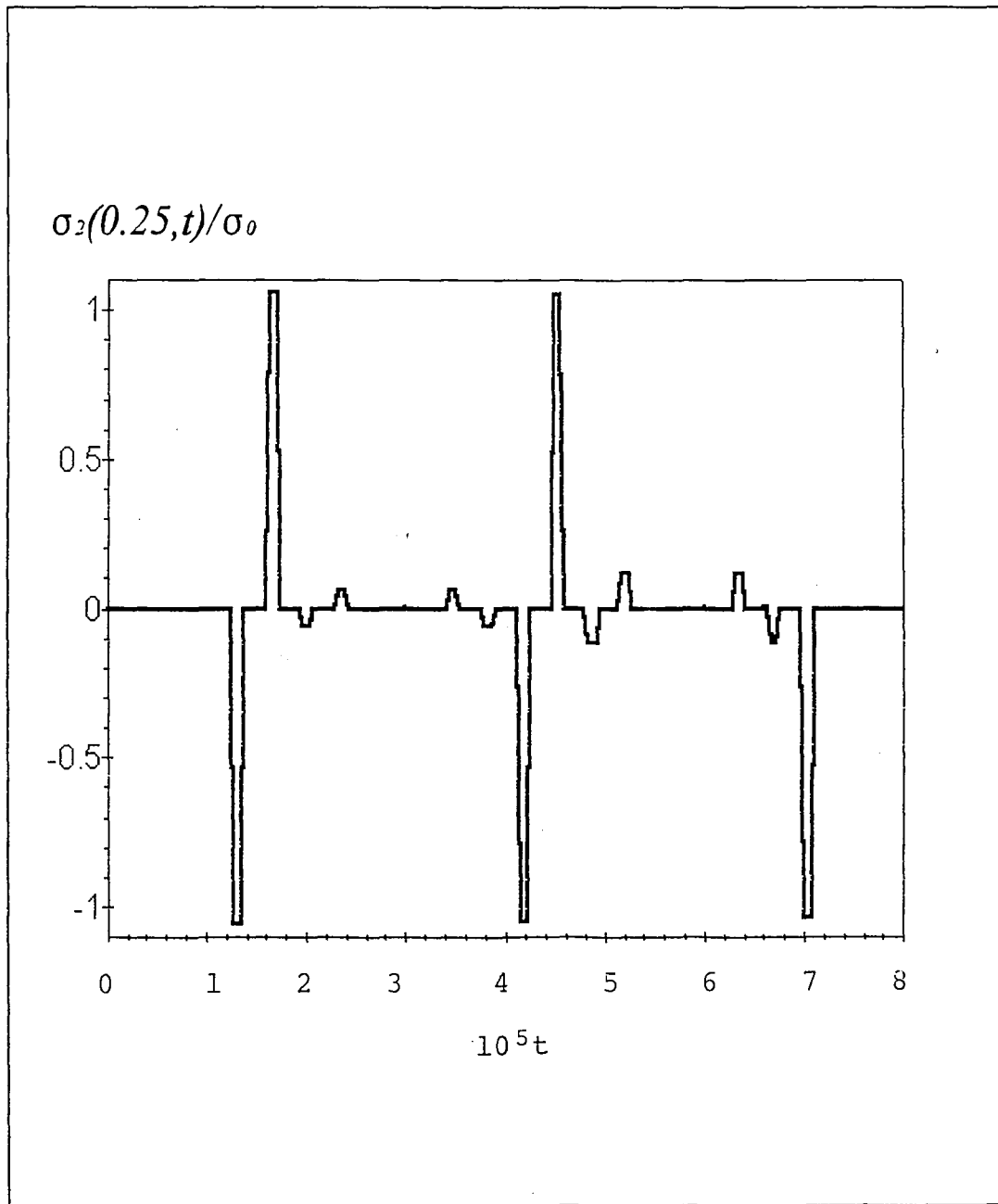


Fig.7 Stress distribution on the middle of material 2(Materials:  
1 Brass, 2 Copper, n=5)

So far we have examined stress distribution in a perfectly bonded two-part composite rod. But practically, every structure contains small flaws, either from manufacture or from the process of fabricating the structure by rolling, machining, punching, or welding. The development of fracture mechanics has shown that fractures initiate from discontinuities of various kind. These discontinuities can vary from extremely small cracks within a weld arc strike to much larger weld or fatigue cracks. Complex welded structures are not fabricated without discontinuities, although good fabrication practice and inspection can minimize the original size and number of these discontinuities. Furthermore even though only small cracks may be present initially, these cracks can grow by stress corrosion or fatigue, possibly to critical size. Thus, to be more practical about the previous study, it is necessary to combine the stress analysis with fracture mechanics\*.

Fracture mechanics technology is based on an analytical procedure that relates the stress-field magnitude and distribution in the vicinity of a crack tip to the nominal stress applied to the structural member, to the size, shape, and orientation of the crack and to material properties. The fundamental

---

\* The concepts of fracture mechanics referred to in this study are based on the references [9]~[12]

principle of fracture mechanics is that the stress field ahead of a sharp crack in a symmetrically loaded structural member can be characterized in terms of a single parameter,  $K$ , the stress intensity factor, that has units of  $\text{ksi}(\text{in})^{1/2}$ .

The stress intensity factor is related to both the nominal stress level in the member and the size of the crack. Thus all structural members, or test specimens, that have flaws can be loaded to various levels of  $K$ , analogous to the situation where unflawed structural members can be loaded to various stress levels. A number of relationships between the stress intensity factor and various body configurations, crack sizes, orientations, and shapes, and loading conditions have been investigated for many years. According to those investigations, the magnitude of the stress intensity factor is directly related to the applied nominal stress level,  $\sigma$ , and the square root of the crack length,  $a$ . In all cases, the general form of the stress intensity factor is given by

$$K = \sigma \sqrt{a} F(t) \quad (36)$$

where  $F(t)$  is a shape function that depends on the specimen and crack geometry as well as the time.

One of the underlying principles of fracture mechanics is that unstable fracture occurs when the stress intensity factor,  $K$  at the crack tip reaches a

critical value,  $K_{Ic}$ .  $K_{Ic}$  is a material parameter called the fracture toughness that depends on the temperature at the crack tip, the rate of loading, and the thickness of the cracked section. It is an experimentally measured quantity that is independent of the crack or structure geometry, of the loading imposed on the structure, and of the crack size. For mode I deformation in which the two fracture surfaces are displaced perpendicular to each other in opposite directions, and for small crack-tip plastic deformation, the critical stress intensity factor for fracture instability is designated  $K_{Ic}$ .  $K_{Ic}$  represents the inherent ability of a material to withstand a given stress intensity at the crack tip and to resist propagation of tensile crack under static loading and plane-strain conditions.  $K_{Ic}$  is a minimum value for thick plates. Material toughness ( $K_{Ic}$ ), crack size ( $a$ ) and stress level ( $\sigma$ ) are three primary factors that control the susceptibility of a structure to fracture. However, it is possible for fracture to occur without all three factors being present if the other factors are sufficiently severe. By knowing the critical value of  $K_{Ic}$  at failure for a given material of a particular thickness and at a specific temperature and loading rate, the allowable stress level that can safely be used for an existing crack can be calculated. In other words,  $K_{Ic}$  should be kept below  $K_{Ic}$  ( under plane-strain conditions ) at all times to prevent

fracture in the design of members with flaws.

However the concept of critical stress intensity factor cannot be used to solve the fracture problem under mixed mode conditions. The energy balance criterion, being a general principle of physics, should apply to this problem.

Fracture will occur when the strain energy release,  $dU/da$  is sufficient to overcome the fracture energy,  $dW/da$ . Hence, the fracture criterion is

$$\left(\frac{dU}{da}\right)_{total} = \frac{dW}{da} \quad (37)$$

$dU/da$  is called the strain energy release rate or, alternatively, the crack driving force. This is conventionally given the symbol  $G$  in the honor of Griffith. The energy balance statement of the critical condition for crack extension is

$$G = G_c \quad (38)$$

where  $G_c$  represents the material resistance against crack propagation, which must be measured experimentally. Thus, crack growth will occur when  $G$

reaches to  $G_c$ .  $G_c$  in a mixed-mode crack extension is greater than in a purely

Mode I crack extension. The increase in the measured  $G_c$  is generally

attributed to yielding at the crack tip region under shear deformation. The

critical energy release for mixed-mode delamination in composite laminate is well presented in [13].

As an example, we will consider the axially symmetric elastostatic problem for an elastic layer which is bonded to a substrate. It will be assumed that there is a penny-shaped crack on the interface the surfaces of which are subjected to known tractions. This is a useful approximation for the delamination problem caused by the reflected plane stress waves in layered materials. The penny-shaped interface crack problem had been solved by Erdogan and Arin [6]. Thus, after adjusting for dynamic effects, we can use the result for the strain energy release rate obtained in [6] (see Fig.8) without any difficulty to solve the problem. In addition, since the stress analysis given in the previous part of this study is still applicable to this problem, we just need to combine the mathematical stress analysis of the loaded system and data for the strain energy release rates shown in Fig.8 under the given conditions to predict the allowable stress level that would prevent failure caused by growth of the crack. To obtain predicted allowable stress level, we are going to take following steps.

1. Obtain the maximum tensile stress on the interface from the dynamic analysis



2. Use the maximum tensile stress to determine the strain energy release rate,  $G$

3. Adjust  $G$  for dynamic effects

4. If  $G$  is smaller than the dynamic fracture toughness,  $G_D$  :

Initial stress applied is allowable

If  $G$  is greater than the dynamic fracture toughness,  $G_D$  :

Crack will grow

Note that for the "impact loading" of a cracked specimen the increase in the stress intensity factor due to dynamic effects is approximately 20%. Since  $G$  is proportional to  $K^2$ , this gives a magnification factor of 1.44 for the strain energy release rate due to dynamic effects.

As an example, we assume that the substrate is 1-inch-thick aluminum and it is coated with 0.01-inch-thick epoxy, and initial stress is applied to the one end of the aluminum substrate with magnitude of  $-\sigma_0$  for  $10^{-7}$  second. Also, we assume that the size of the penny-shaped crack which exist on the interface is 0.01 inch. The elastic properties of aluminum and epoxy are shown in Table 2. By the Maple program we have made before, the plots(Fig.9~19) showing stress distributions on the interface when  $n=0,1,2,3,4,5,6,7,8,9,10$  respectively are obtained. Fig.20 is partly magnified

Fig.19. Examining Fig.19, we can see that stress distribution on the interface is in the range from  $-0.24\sigma_0$  to  $0.42\sigma_0$ . Thus, the maximum tensile stress on the interface is  $0.42\sigma_0$ . Now we need to calculate the strain energy release rate for the interface crack corresponding to the maximum tensile stress obtained. From Fig.8, we obtain  $10^5(dU/da)/p_0^2a = 0.32$  for  $h/2a=1$ . Because  $p_0=0.42\sigma_0$  and  $a=0.005$  are known values, we can easily calculate the strain energy release rate,  $G$ .

$$G = 0.32p_0^2a \times 10^{-5} = 0.32 \times 0.42^2 \times 0.005 \times 10^{-5} \times \sigma_0^2 = 0.282 \times 10^{-8} \sigma_0^2$$

Adjusting  $G$  for dynamic effects gives

$$G = 1.44 \times 0.282 \times 10^{-8} \times \sigma_0^2 = 0.406 \times 10^{-8} \sigma_0^2$$

If  $G_D$  which can be determined experimentally is greater than  $0.406 \times 10^{-8} \sigma_0^2$ , the crack on the interface will not grow. If  $G_D$  is smaller than  $0.406 \times 10^{-8} \sigma_0^2$ , we have to reduce the allowable stress level to prevent failure.

Fig.21 and Fig.22 show the stress distribution (same Aluminum-Epoxy bonding) at the location of  $x = +h_2/10$ ,  $x = -h_2/10$  respectively. These plots can be used when we consider the fractures which occur at the location of

$x=\pm h_2/10$ (other than the interface).

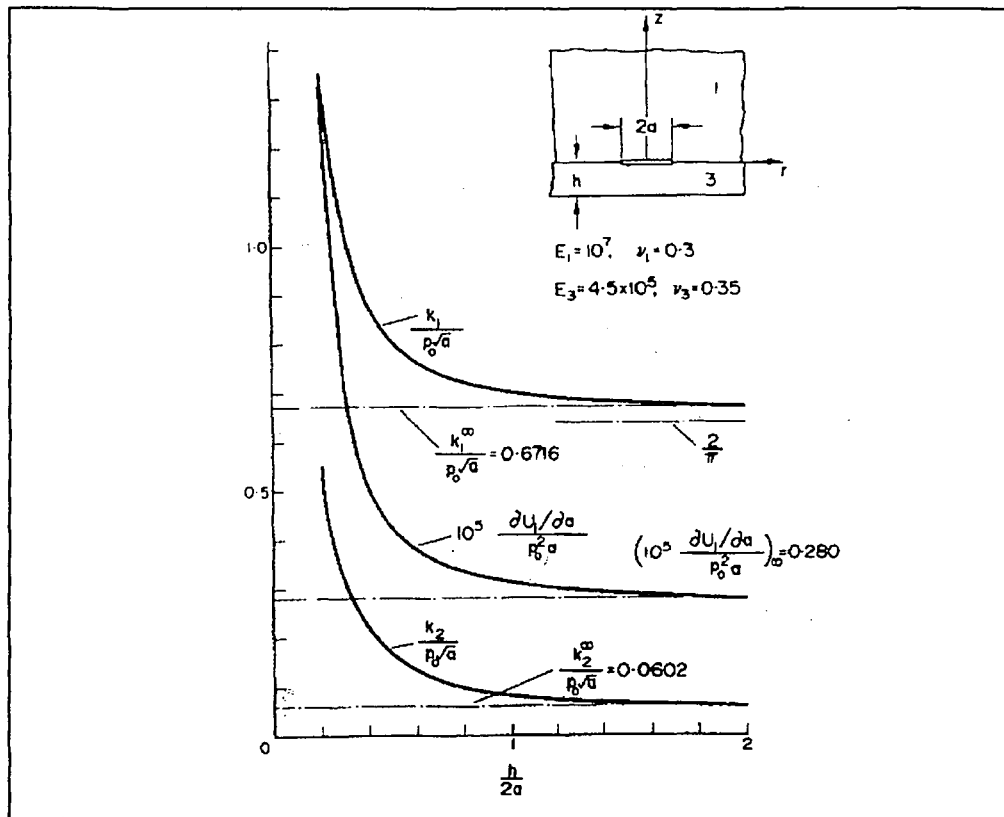


Fig.8 Stress intensity factors and the strain energy release rate for a penny-shaped interface crack(Materials: 1 Aluminum, 2 Epoxy)\*

	E(psi)	$\rho$ (lb/in <sup>3</sup> )	c(in/sec)	h(inch)
Material 1(Aluminum)	$10^7$	0.1	196501.9	$h_1$
Material 2(Epoxy**)	$4.5 \times 10^5$	0.042	64320.3	$h_2$

Table 2 Elastic constants of Aluminum and Epoxy

\* From reference [6]

\*\* From reference [15]

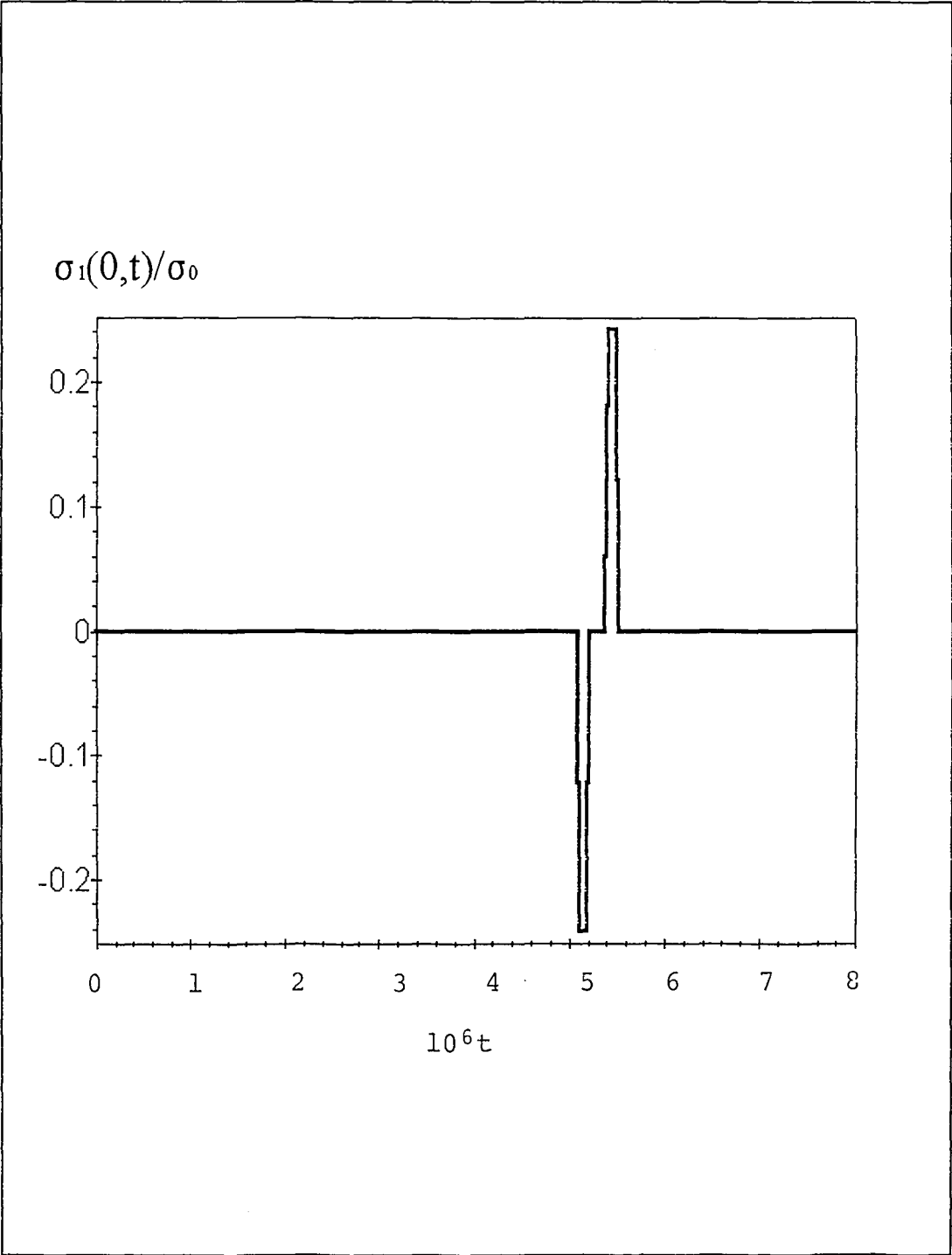


Fig.9 Stress distribution on the interface(Materials: 1 Aluminum, 2 Epoxy,  $n=0$ )

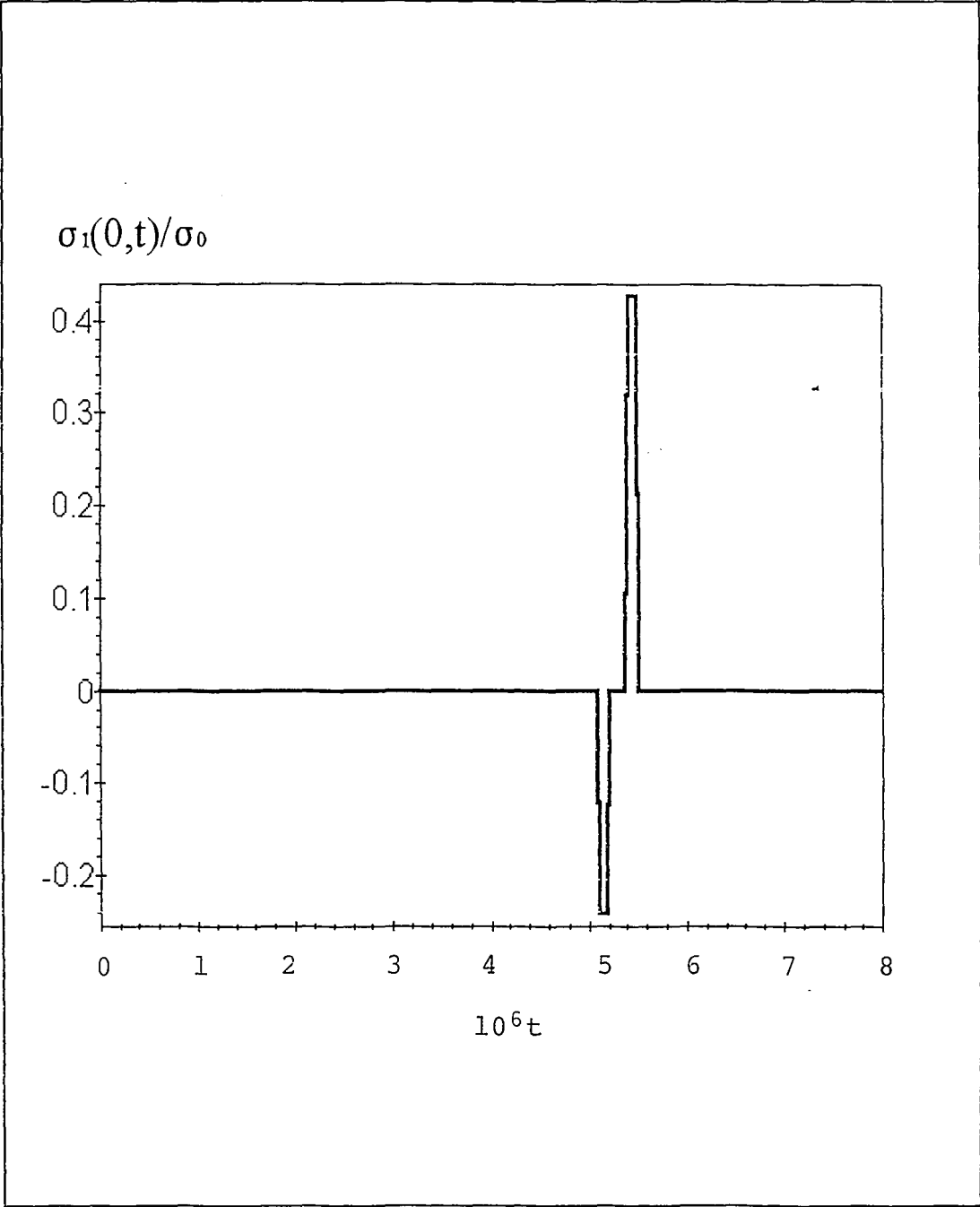


Fig.10 Stress distribution on the interface(Materials: 1 Aluminum, 2 Epoxy, n=1)

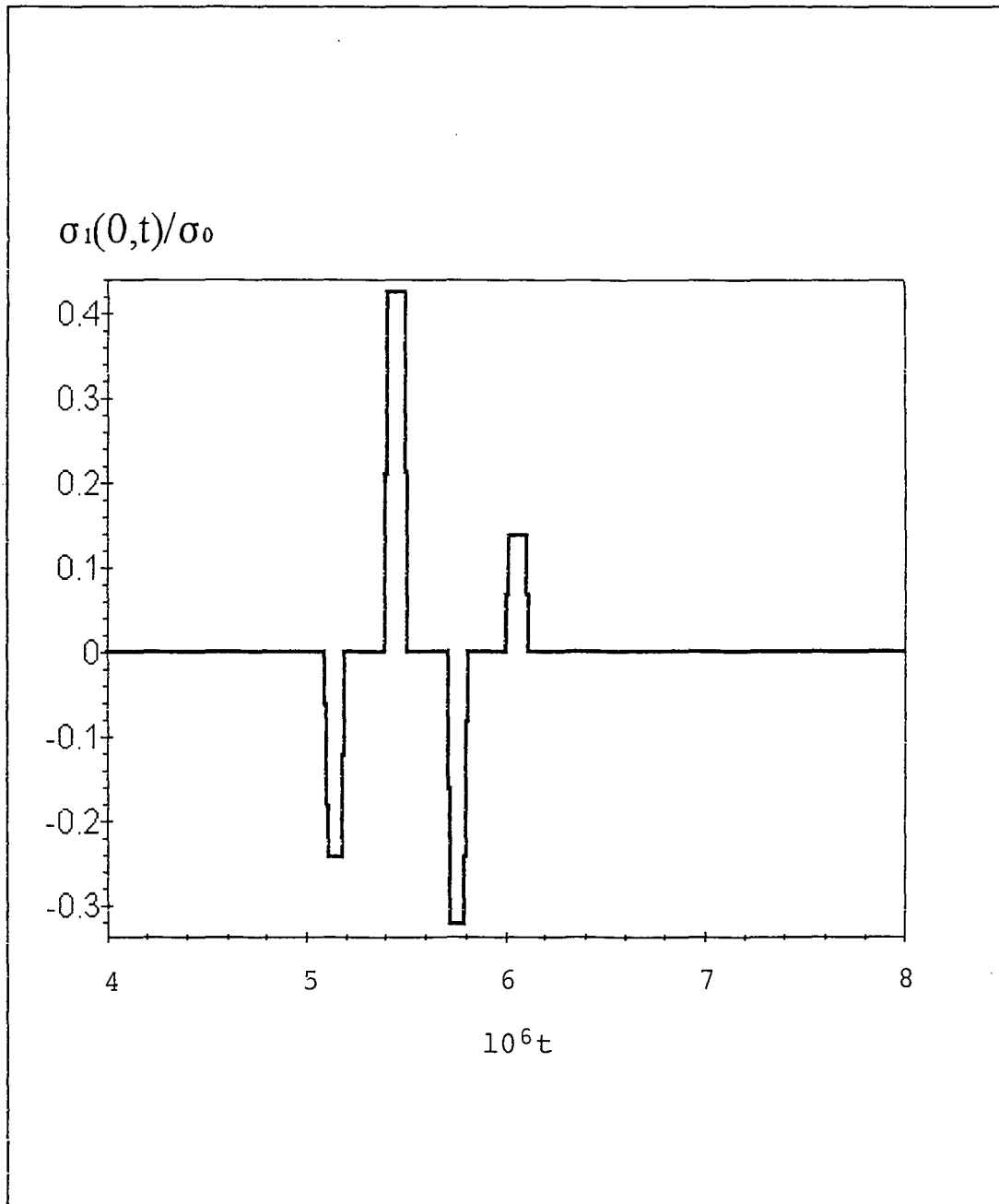


Fig.11 Stress distribution on the interface(Materials: 1 Aluminum,  
2 Epoxy, n=2)

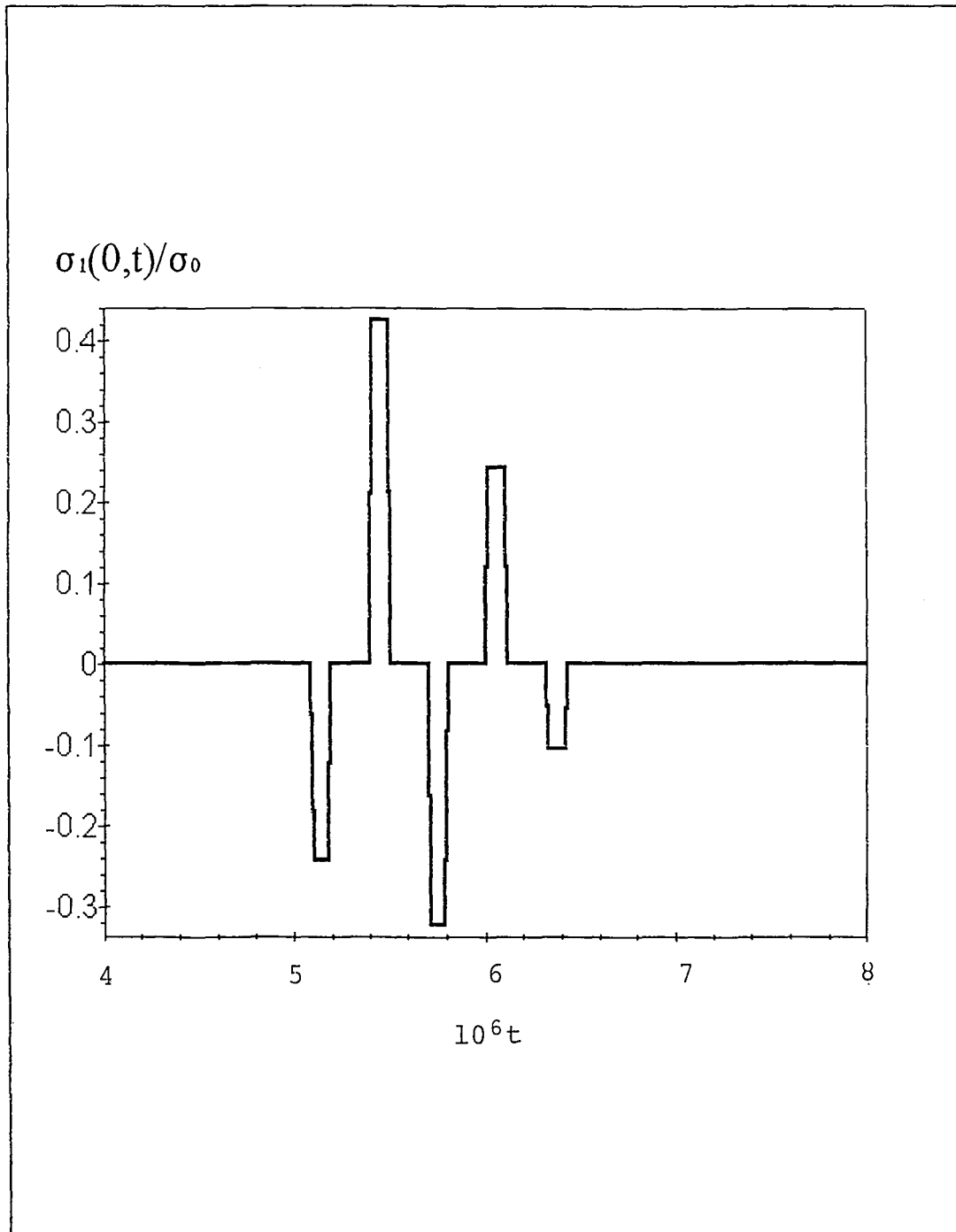


Fig.12 Stress distribution on the interface(Materials: 1 Aluminum,  
2 Epoxy,  $n=3$ )

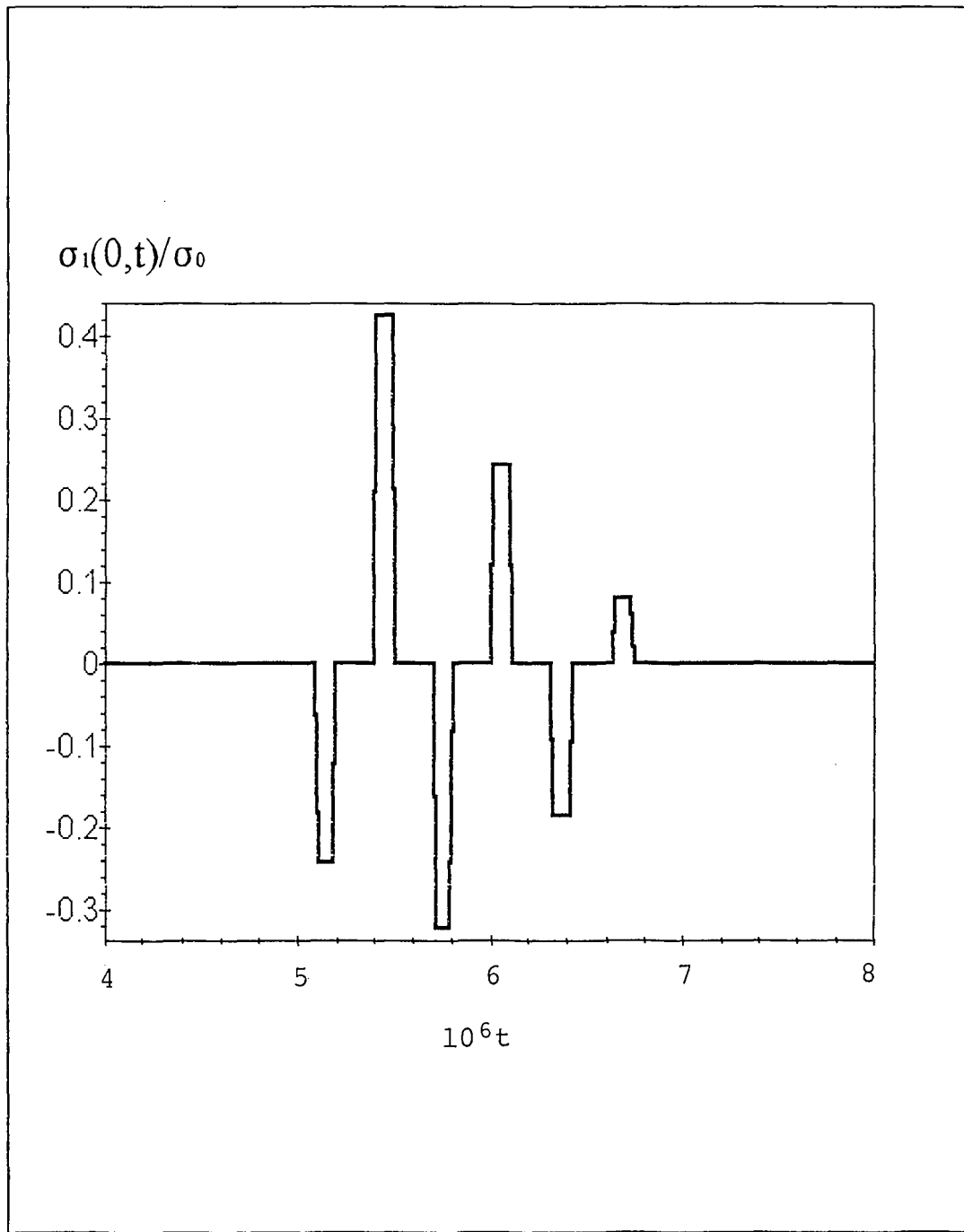


Fig.13 Stress distribution on the interface(Materials: 1 Aluminum, 2 Epoxy, n=4)



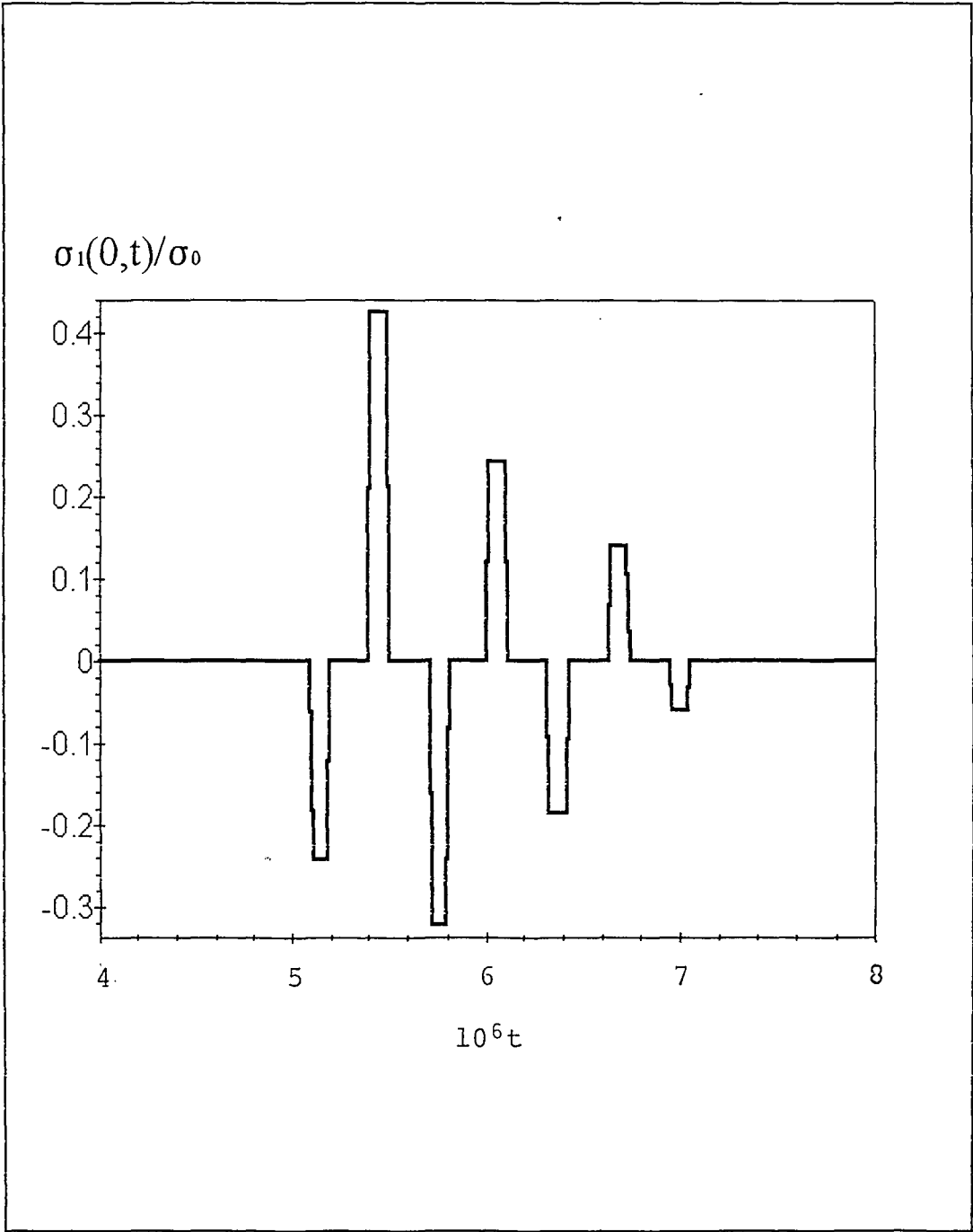


Fig.14 Stress distribution on the interface(Materials: 1 Aluminum, 2 Epoxy, n=5)

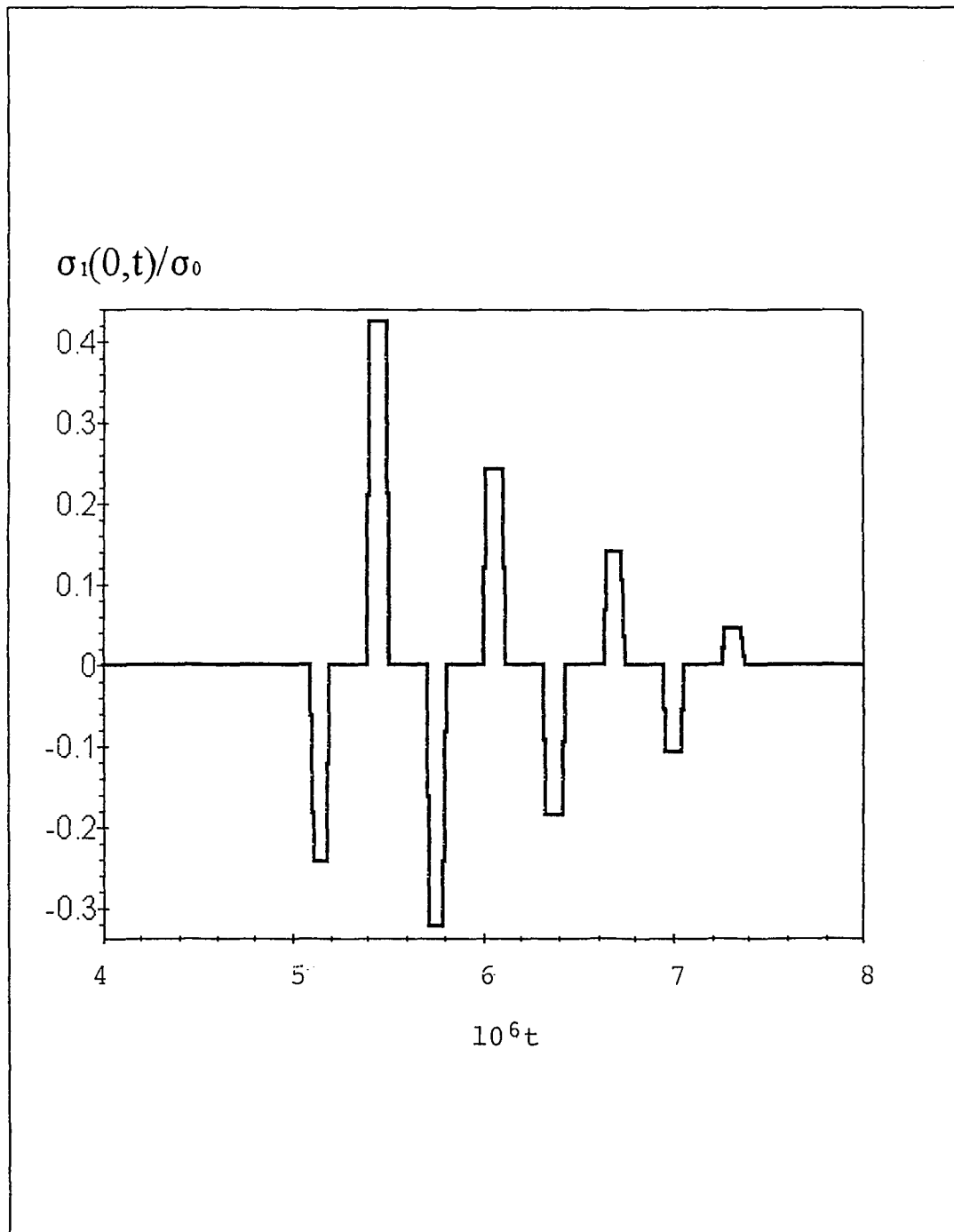


Fig.15 Stress distribution on the interface(Materials: 1 Aluminum, 2 Epoxy, n=6)

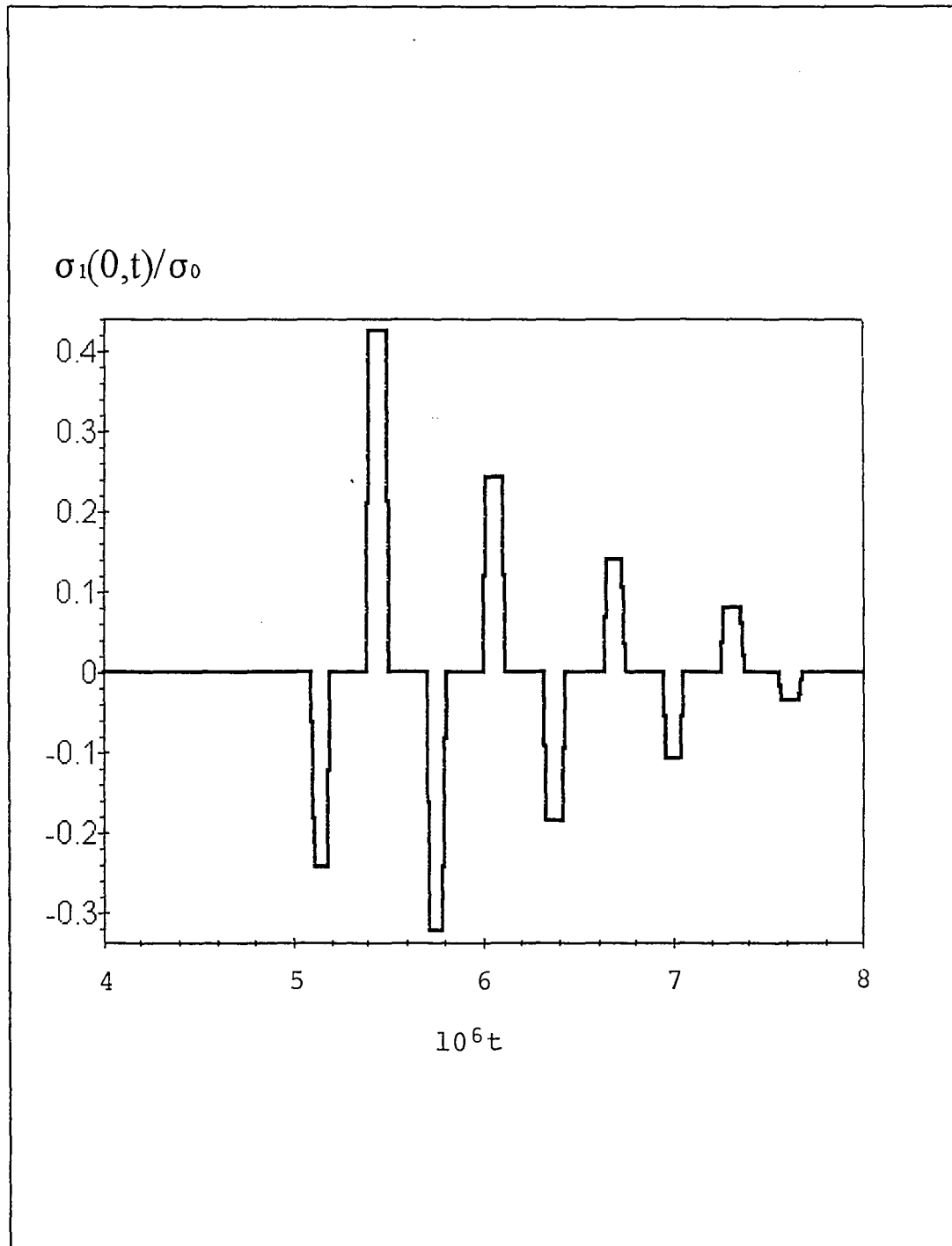


Fig.16 Strss distribution on the interface(Materials: 1 Aluminum, 2 Epoxy, n=7)

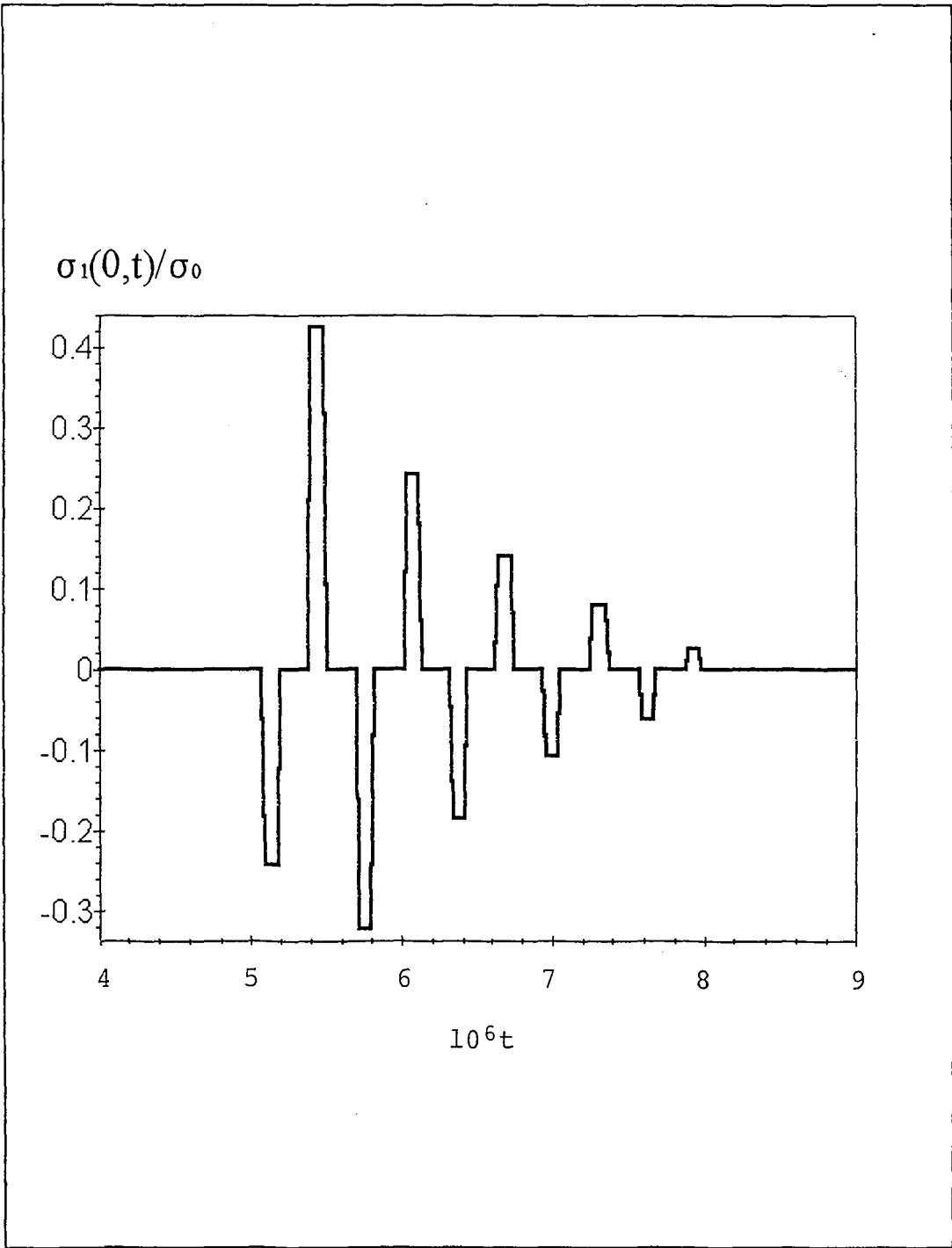


Fig.17 Stress distribution on the interface(Materials: 1 Aluminum, 2 Epoxy, n=8)

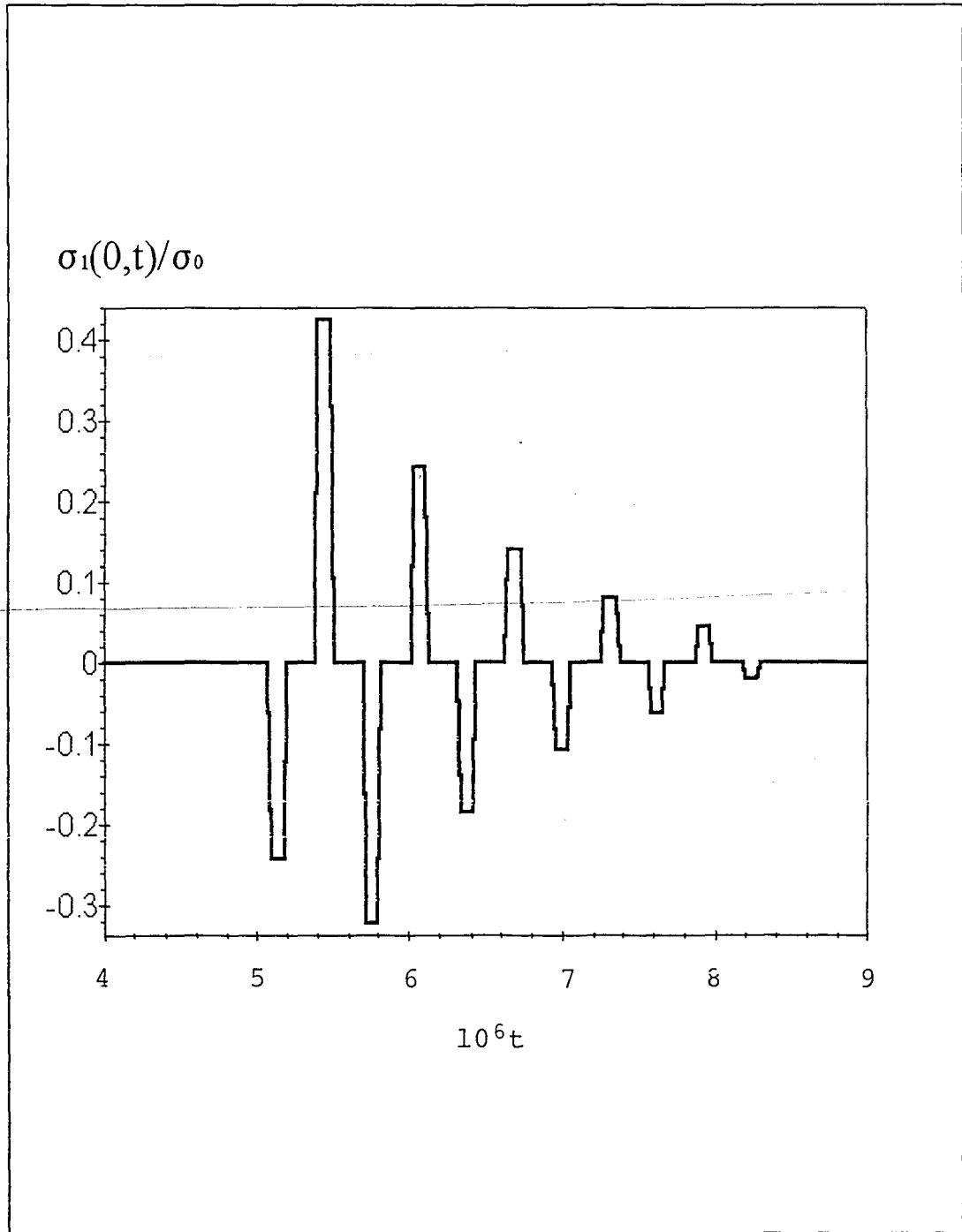


Fig.18 Stress distribution on the interface(Materials: 1 Aluminum,  
2 Epoxy, n=9)

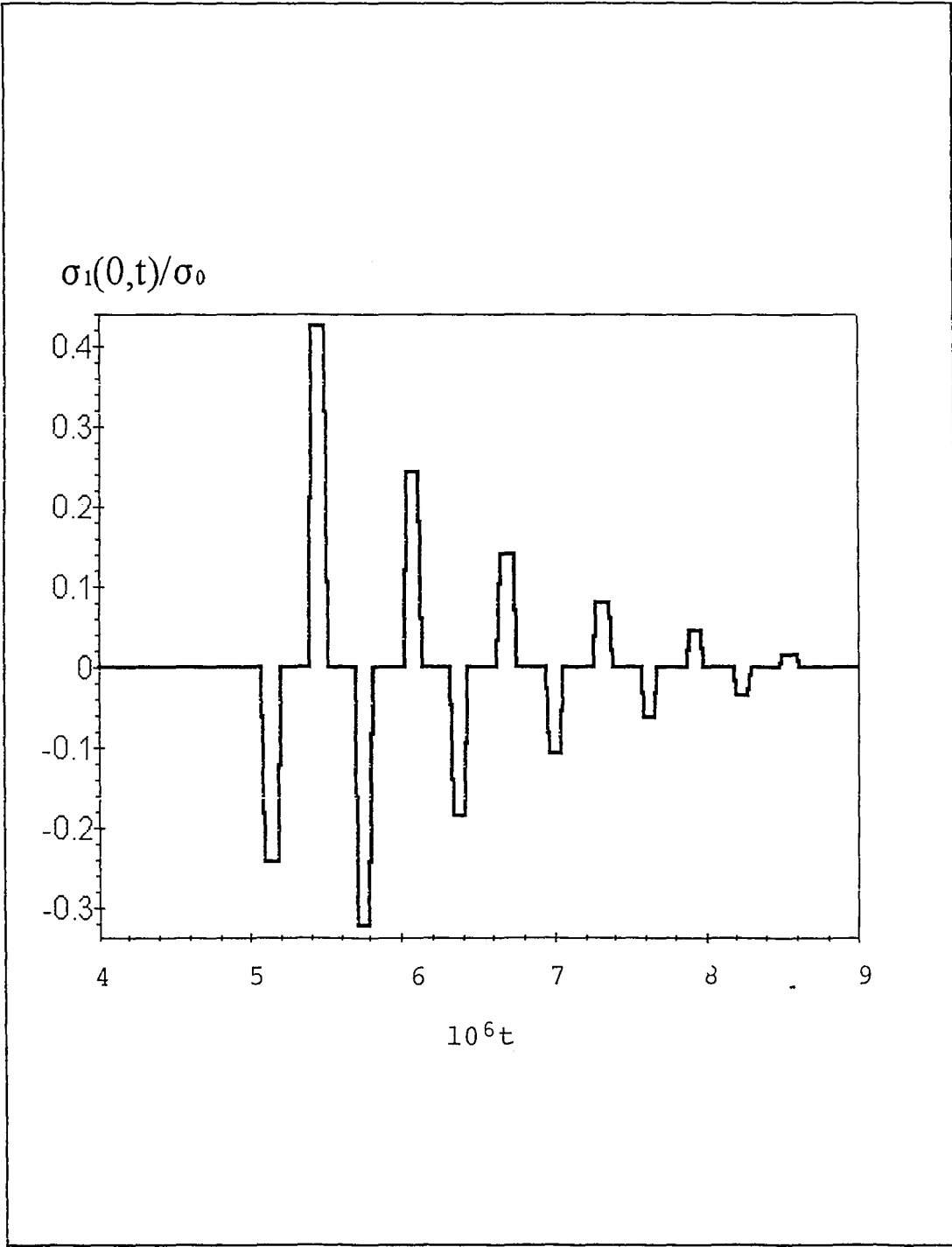


Fig 19 Stress distribution on the interface(Materials: 1 Aluminum, 2 Epoxy, n=10)

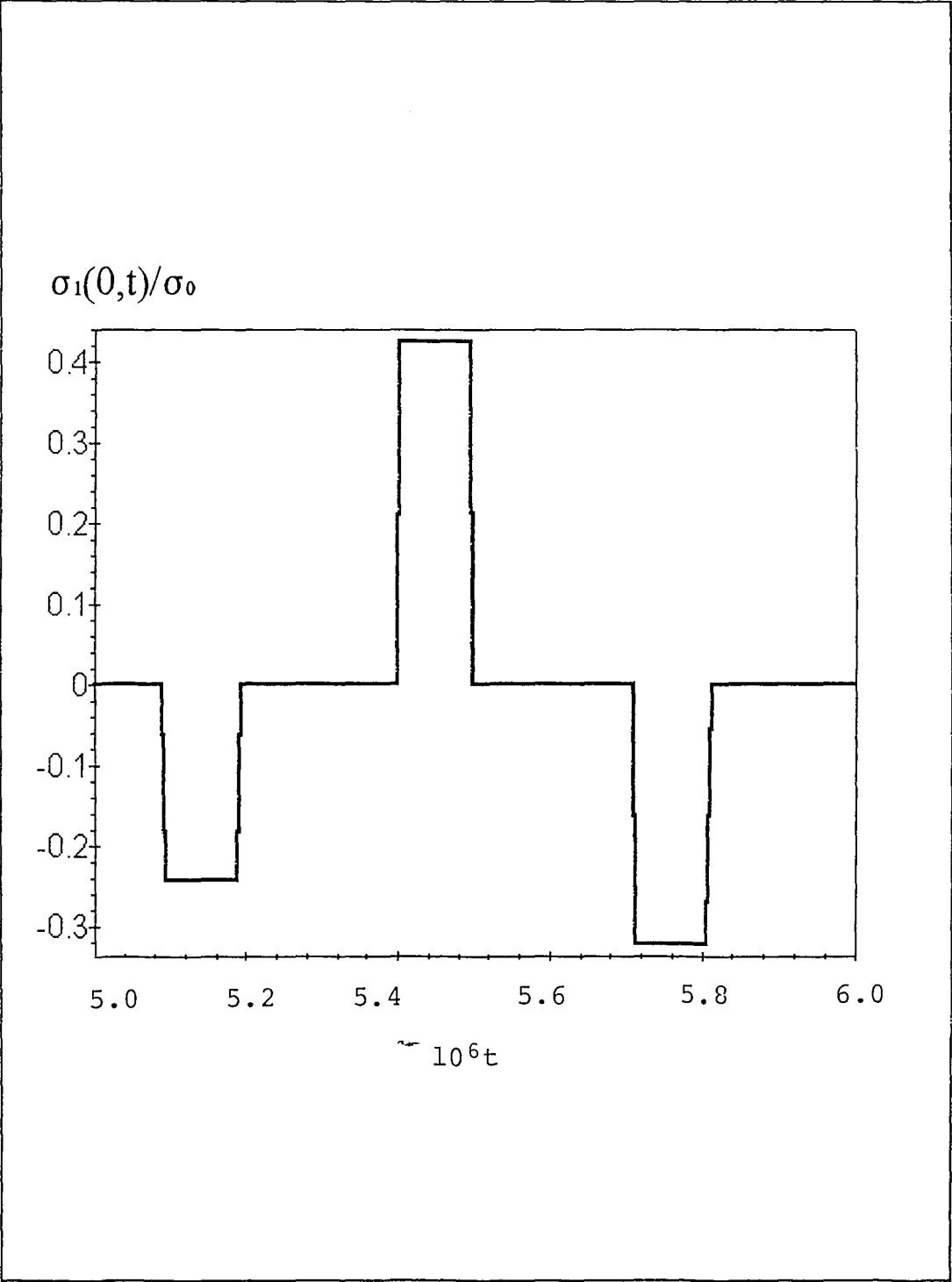


Fig.20 Partly magnified plot of Fig.19

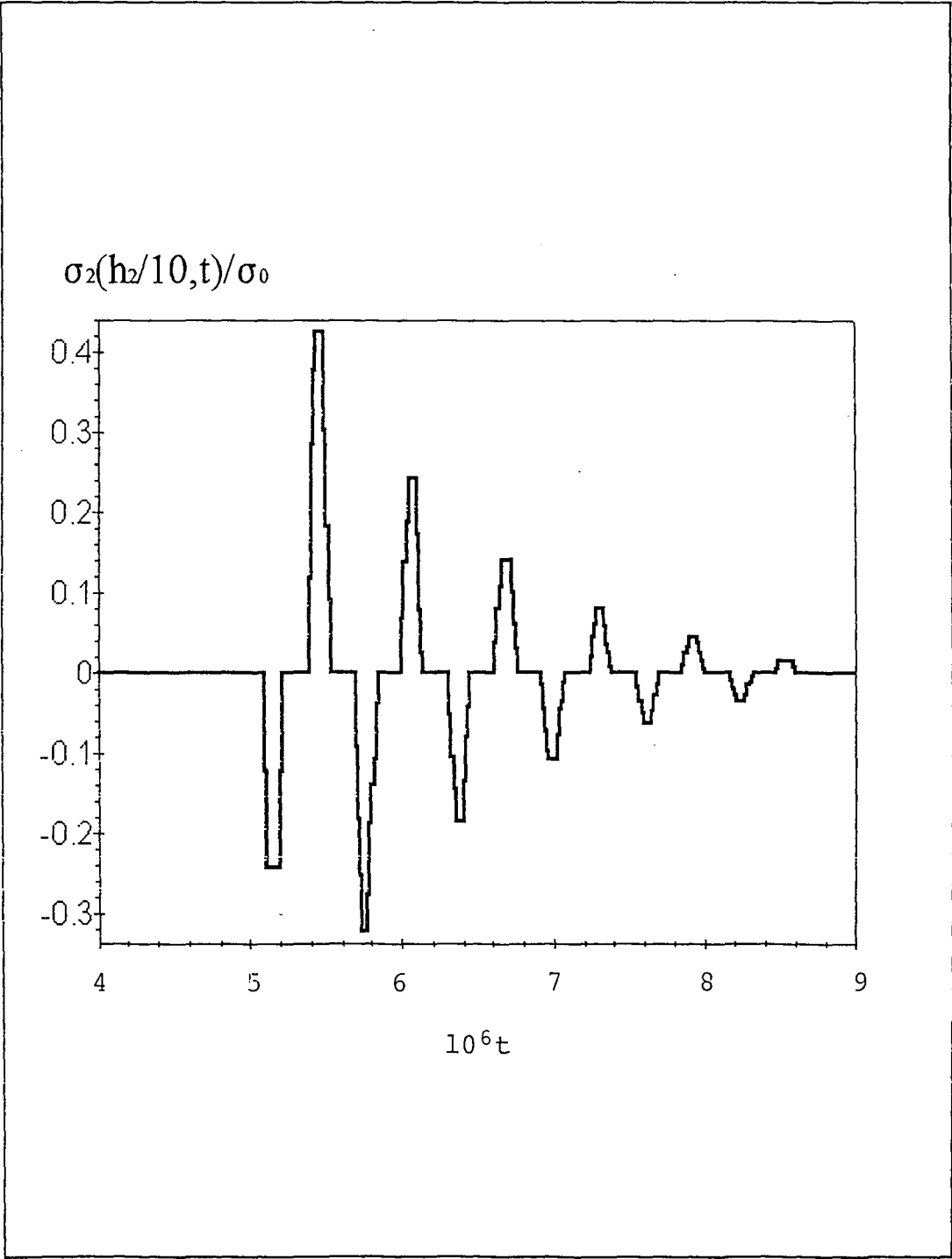


Fig.21 Stress distribution at  $x=h_2/10$ (Materials: 1 Aluminum, 2 Epoxy,  $n=10$ )



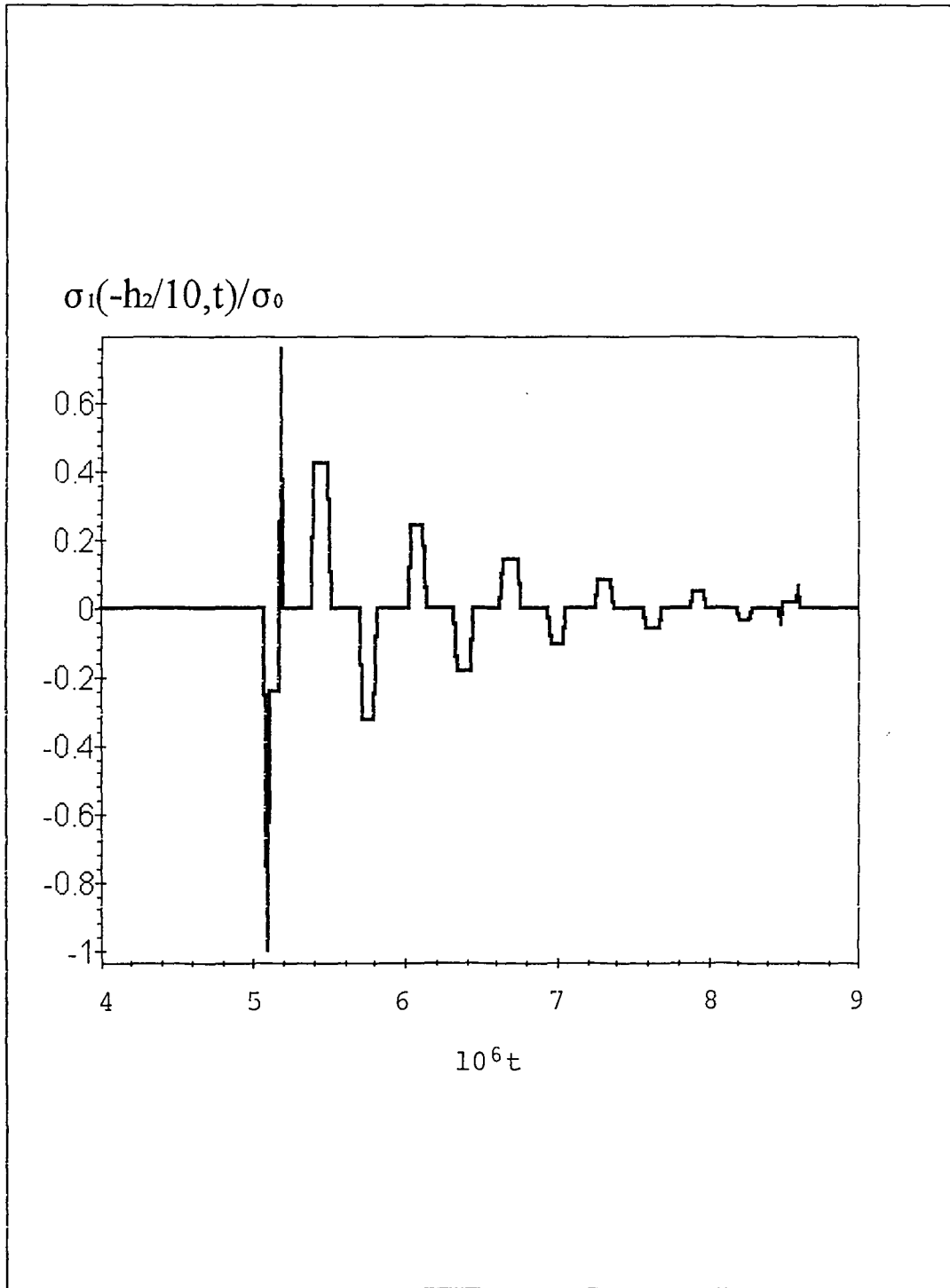


Fig.22 Stress distribution at  $x=-h_2/10$ (Materials: 1 Aluminum, 2 Epoxy,  $n=10$ )

## 4. Conclusions

Mathematical stress analysis on the interface of coated elastic medium is presented. The solution obtained can be used to solve the delamination problem of coated materials.

In addition, since we can obtain the stress distribution at any location other than interface, our study may be extended to consider the problem of fracture propagation that may take place at an arbitrary location in the coating or the substrate. For this kind of problem, we need to combine the tensile stress at a critical location in the coating or substrate with data of strain energy release rate and the fracture toughness corresponding to the particular material.

## References

- [1] H. Kolsky, Stress Waves in Solids, Dover Publications(1963)
- [2] B. W. Abbott and R. H. Cornish, "A Stress Wave Technique for Determining the Tensile Strength of Brittle Materials", Exp. Mech.(1965)
- [3] B. W. Abbott and L. J. Broutman, "Stress-Wave Propagation in Composite Materials", Exp. Mech.(1966)
- [4] K. Arin and F. Erdogan, "Penny-Shaped Crack in an Elastic Layer Bonded to Dissimilar Half Spaces", Int. J. Engng Sci.(1971)
- [5] F. Erdogan and G. D. Gupta, "Layered Composites with an Interface Flaw", Int.J. Solids Structures(1971)
- [6] F. Erdogan and K. Arin , "Penny-Shaped Interface Crack between an Elastic Layer and a Half Space", Int. J. Engng Sci.(1972)
- [7] Vijay Gupta, Jun Yuan and Alexander Pronin, "Recent Developments in the Laser Spallation Technique to Measure Interface Strength", J. Adhesion Sci. Technol.(1994)
- [8] Karl. F. Graff, Wave Motion in Elastic Solids,Dover Publications(1991)
- [9] David K. Felbeck and Anthony G. Atkins, Strength and Fracture of Engineering Solids, Prentice Hall(1984)
- [10] John M. Barsom and Stanley T. Rolfe, Fracture and Fatigue Control in Structures, Prentice-Hall International Series(1987)
- [11] David Broek, The Pratical Use of Fracture Mechanics, Kluwer Academic Publishers(1989)
- [12] Melvin F. Kanninen and Carl H. Popelar, Advanced Fracture Mechanics, Oxford(1985)
- [13] A. S. D. Wang, M. Slomiana and R. B. Bucinell, "Delamination Crack Growth in Composite Laminates", ASTM(1985)

[14] Henry R. Clauser, Editor, Encyclopedia/Handbook of Materials, Parts and Finishes, Technomic Publishing(1976)

[15] George S. Brady and Henry R. Clauser, Material Hand Book, McGraw-Hill(1986)

## VITA

Jung-ho Kim was born in 1966.

His parents, Myung-kwan Kim and Bok-nam Kim had brought him up in the city of Pusan, South Korea since his birth. B.S. degree was conferred to him from Pusan National University in 1985. After graduation, he had worked for a textile company for two years as an assistant manager. He has been studying at Lehigh University since 1993.

**END OF  
TITLE**